Evolution, 2025, **79(1)**, 100–118
https://doi.org/10.1093/evolut/qpae143
Advance access publication 09 October 2024
Original Article

Coevolution promotes the coexistence of Tasmanian devils and a fatal, transmissible cancer

Dale T. Clement[1], Dylan G. Gallinson[2], Rodrigo K. Hamede[3,4], Menna E. Jones[3], Mark J. Margres[2], Hamish McCallum[5] and Andrew Storfer[6]

[1]Department of Biology, Wake Forest University, Winston-Salem, NC, United States
[2]Department of Integrative Biology, University of South Florida, Tampa, FL, United States
[3]School of Natural Sciences, University of Tasmania, Hobart, TAS, Australia
[4]CANECEV: Centre de Recherches Ecologiques et Evolutives sur le Cancer, Montpellier, France
[5]Centre for Planetary Health and Food Security, Griffith University, Nathan Campus, Nathan, Queensland, Australia
[6]School of Biological Sciences, Washington State University, Pullman, WA, United States

Corresponding authors: Department of Biology, Wake Forest University, 1834 Wake Forest Road, Winston-Salem, NC 27109, United States. Email: clemend@wfu.edu; School of Biological Sciences, Washington State University, Pullman, WA 99164, United States. Email: astorfer@wsu.edu

Abstract

Emerging infectious diseases threaten natural populations, and data-driven modeling is critical for predicting population dynamics. Despite the importance of integrating ecology and evolution in models of host–pathogen dynamics, there are few wild populations for which long-term ecological datasets have been coupled with genome-scale data. Tasmanian devil (*Sarcophilus harrisii*) populations have declined range wide due to devil facial tumor disease (DFTD), a fatal transmissible cancer. Although early ecological models predicted imminent devil extinction, diseased devil populations persist at low densities, and recent ecological models predict long-term devil persistence. Substantial evidence supports the evolution of both devils and DFTD, suggesting coevolution may also influence continued devil persistence. Thus, we developed an individual-based, eco-evolutionary model of devil–DFTD coevolution parameterized with nearly 2 decades of devil demography, DFTD epidemiology, and genome-wide association studies. We characterized potential devil–DFTD coevolutionary outcomes and predicted the effects of coevolution on devil persistence and devil–DFTD coexistence. We found a high probability of devil persistence over 50 devil generations (100 years) and a higher likelihood of devil–DFTD coexistence, with greater devil recovery than predicted by previous ecological models. These novel results add to growing evidence for long-term devil persistence and highlight the importance of eco-evolutionary modeling for emerging infectious diseases.

Keywords: Tasmanian devil, eco-evolutionary dynamics, host–pathogen coevolution, disease ecology, individual-based model, quantitative genetics

Introduction

Emerging infectious diseases (EIDs) are a leading threat to natural populations. EIDs have directly caused the extinction of many species (Fisher et al., 2012) and contributed to the decline of numerous others (De Castro & Bolker, 2005b; Jones et al., 2008). The epidemiological outcome of an EID, ranging from local host extirpation to pathogen extirpation to forms of coexistence and disease endemism, results from a complex interplay of both ecological and coevolutionary processes (McKnight et al., 2017; Vander Wal et al., 2014a). By creating in silico experiments that would be impossible to conduct in the field or lab, data-driven modeling plays an important role in predicting how ecology and coevolution interact to drive the outcomes of EIDs. Evolution regularly occurs on ecological timescales, particularly for pathogens (Hairston et al., 2005; Hendry & Gonzalez, 2008; Hendry et al., 2018), and the study of "eco-evolutionary dynamics" over the past two decades (Post & Palkovacs, 2009; Reznick et al., 2019; Schoener, 2011) has facilitated efforts to combine epidemiological and coevolutionary theory (Boots et al., 2009; Lively, 2010, 2016; Vander Wal et al., 2014a). However, there is still a pressing need to apply this theory to species of conservation concern (Brannelly et al., 2021; Shefferson et al., 2018; Smith et al., 2014; Vander Wal et al., 2014a).

Epidemiological theory predicts that patterns of pathogen transmission strongly affect the likelihood that an EID results in population extirpation. For many pathogens, the rate of transmission decreases with host density, which leads to disease fadeout rather than host extirpation, as host populations decline over the course of an epidemic (McCallum et al., 2001). However, if pathogen transmission is independent of host density (e.g., sexually transmitted diseases, where transmission is strongly coupled with host mating behavior), the resulting frequency-dependent transmission may drive populations to extinction (De Castro & Bolker, 2005a; McCallum et al., 2001). High disease-related mortality often leads to rapid population collapse during an epizootic outbreak (Vredenburg et al., 2010) or slow population decline and

Received April 24, 2024; revisions received September 19, 2024; accepted October 04, 2024
Associate Editor: Ben Ashby; Handling Editor: Jason Wolf

extinction for endemic pathogens that reduce host per-capita reproduction below replacement (Valenzuela-Sánchez et al., 2017). Notably, many high-profile EIDs responsible for mass population declines are characterized by high disease-related mortality (e.g., chytrid, Lips et al., 2006; white-nose syndrome; Hoyt et al., 2021).

Rapid evolution can dramatically affect the outcome of a disease outbreak; there are many documented cases of evolution "rescuing" natural populations from disease-induced extinction (most prominently in biocontrol, e.g., the initial stages of the myxoma epizootic in Australian rabbits; reviewed in Kerr, 2012). The effect of evolution depends on which traits are under selection. The evolution of host resistance (reduced susceptibility) and host tolerance (reduced disease-related mortality) are both predicted to reduce the likelihood of host extirpation. However, the evolution of resistance is predicted to decrease disease prevalence while the evolution of tolerance promotes greater disease prevalence and host–pathogen coexistence (Roy & Kirchner, 2000; reviewed in Searle & Christie, 2021). Though disease evolution may in some cases synergize with host evolution to promote host persistence (many highly virulent EIDs have evolved reduced virulence during the initial disease outbreak; Bolker et al., 2010; e.g., myxoma virus, Kerr, 2012), rapid coevolution of both host and pathogen may also lead to host extirpation or a long-term reduction in host abundance. For example, the phenotypic difference model, a common quantitative trait model of coevolution, assumes that a disease-related trait (usually infectivity or the fitness cost of infection) is a function of the difference between the host and pathogen genotype and predicts arm race dynamics between-host resistance and pathogen transmissibility whereby the "losing" species is extirpated (Nuismer, 2017). Additionally, myxoma virus evolved greater virulence in the decades following the evolution of rabbit resistance (Kerr et al., 2017, 2022), and rabbit abundance still remains well below its pre-myxoma high (Saunders et al., 2010). The effect of multivariate coevolution is even more complex, with evolutionary outcomes depending on the infection rate, background mortality, trait fitness costs, among other factors (e.g., Carval & Ferriere, 2010).

Despite the growing body of theory, there are still few eco-evolutionary models of host–pathogen coevolution in species of conservation concern. Long-term ecological datasets on host–pathogen dynamics necessary to parameterize such models are rare but becoming more common (e.g., Byrne et al., 2019; Epstein et al., 2016). Given that rapid evolution frequently alters ecological dynamics (and vice versa), integrating the two data types in eco-evolutionary models is critical in an era when EIDs increasingly threaten species persistence and risk spillover to humans and livestock (Hohenlohe et al. 2019; Vander Wal et al. 2014a, 2014b).

The Tasmanian devil (*Sarcophilus harrisii*) has experienced range-wide population declines of approximately 80% due to the devil facial tumor disease (DFTD), a fatal transmissible cancer. DFTD has generated a "natural experiment" of an EID that has spread predictably east-to-west across nearly all the devil's known geographic range over the past ~25 years (Cunningham et al., 2021; Lazenby et al., 2018; Storfer et al., 2018). This system has been the subject of extensive, long-term collection of both ecological and genetic data (e.g., Cunningham et al., 2021; Epstein et al., 2016; Lazenby et al., 2018; Strickland et al., 2024). DFTD is transmitted by biting during frequent social interactions, such as aggregation at carcasses during scavenging and mate guarding (Hamede et al., 2008, 2013; Hamilton et al., 2019), and hence has a strong frequency-dependent component to transmission. Initial compartmental epidemiological models (Beeton & McCallum, 2011; McCallum et al., 2009) predicted devil extinction due to this frequency-dependent transmission and DFTD's high virulence.

However, all continuously distributed diseased devil populations have persisted at low-to-medium densities (Lazenby et al., 2018), and more recent models predict continued devil persistence in the majority of scenarios (Siska et al., 2018; Wells et al., 2019), likely because most infected individuals survive to breed in the next breeding season with no vertical transmission to offspring (Lazenby et al., 2018; Wells et al., 2017). Moreover, these models are based only on ecological mark–recapture data. Evidence of evolution in both devils (Epstein et al., 2016; Fraik et al., 2020; Stahlke et al., 2021) and tumors (Kwon et al., 2020; Patton et al., 2020; Stammnitz et al., 2023) suggests rapid evolution could affect devil persistence. Devil genetic variation explains a significant proportion of phenotypic variance in survival after infection (Margres et al., 2018) and infection status (Margres et al., 2018; Strickland et al., 2024). Time series analyses of devil populations pre- and post-DFTD emergence show evidence of rapid evolutionary responses to selection in genomic regions containing immune-related genes (Epstein et al., 2016; Hubert et al., 2018; Stahlke et al., 2021). DFTD also has evolved into four genetically distinct lineages (Kwon et al., 2020; Patton et al., 2020; Stammnitz et al., 2023) and shown local variation in tumor genetic diversity over time (Hamede et al., 2023). DFTD's effective reproduction rate R_e—equivalent to transmission—declined from 3.5 during the exponential growth phase to ~1, or replacement, at present, suggesting the potential evolution of DFTD toward endemism (Patton et al., 2020). Gallinson et al. (2024) found that the interaction between devil and tumor genomes explained a significant proportion of variation in force of infection (FOI; measured by proxy as the number of days a susceptible individual takes to become infected with DFTD), and identified devil and tumor genes associated with this variation. Taken together, these studies provide substantial evidence suggesting devil–DFTD coevolution in multiple disease-related traits.

However, not all traits may be as likely to evolve and it is still unclear how coevolution in different traits will impact long-term devil persistence. We expect strong coevolution between devil resistance to infection and DFTD transmissibility, as these traits have substantial underlying genetic variation (Gallinson et al., 2024; Margres et al., 2018; Strickland et al., 2024). Similarly, genetic variation in devil survival indicates the possibility for the evolution of increased devil tolerance (Margres et al., 2018), though no empirical study has yet examined among lineage variation in DFTD virulence. If coevolution of DFTD virulence and devil tolerance is present, the expected outcome would be lower devil mortality and a substantial, positive effect on devil persistence and devil–DFTD coexistence (Berngruber et al., 2013; Bolker et al., 2010). Coevolution of host resistance and pathogen transmissibility, on the other hand, could lead to arms race dynamics, the outcome of which would depend on the relative rates of host and pathogen evolution (e.g., if coevolution follows the phenotypic difference model; Nuismer, 2017). Given

the decline in DFTD transmission toward replacement, it is possible an arms race dynamic would favor devils (Hamede et al., 2023; Patton et al., 2020).

Thus, it is necessary to develop an eco-evolutionary model to investigate the consequences of evolutionary dynamics for long-term devil–DFTD population dynamics and we have a unique combination of long-term mark–recapture data and genomic analyses that make it feasible to parameterize such a model. Herein, we present one of the first studies to model the effect of rapid coevolution on population extirpation risk due to an EID. We ask three questions: (a) In which traits do devil–DFTD coevolution result in patterns of life history, infection, and evolution consistent with empirical data? (b) How does coevolution affect the probability of devil persistence and devil–DFTD coexistence relative to a non-evolving population? (c) In which traits is coevolution most important for driving devil persistence and devil–DFTD coexistence? To answer these questions, we developed an individual-based, eco-coevolutionary model of devil–DFTD dynamics with coevolution in three pairs of DFTD and devil traits: (a) the probability of tumor transmission and devil resistance to infection; (b) tumor growth rate on an infected individual and devil resistance to growth; (c) tumor virulence and devil tolerance (following the definitions of Råberg et al., 2009). Via model parameterization, we first predict which traits are most likely to be coevolving and, second, we use simulations to test how—and in which traits—coevolution affects the probability of devil and DFTD persistence to 50 generations (100 years; following Wells et al., 2019).

Methods

Model description

We present an individual-based eco-evolutionary model of the devil population and DFTD epidemiological dynamics with discrete, weekly timesteps. DFTD epidemiology follows a susceptible-exposed-infected (SEI) framework. The infected class is structured by tumor size, with larger tumors having a higher probability of transmission and causing higher mortality than smaller tumors. We focus on coevolution in three "realized" disease-related traits: (a) The realized resistance of susceptible individual i to infection by infected individual j (R_{ij}) which affects the probability individual i remains uninfected P_{ij}^{S} in each timestep, (b) The realized tumor growth rate r_i^{growth} for infected individual i, and (c) The "critical tumor load for survival" (see below) of infected individual i ($L_{S,i}^{crit}$), which affects weekly survival probability P_i^{surv}. Coevolution follows the phenotypic difference model such that each realized trait k is a function of the difference between the latent quantitative devil trait ($z_{k,i}$) and latent quantitative tumor trait ($x_{k,i}$ or $x_{k,j}$ depending on whether the trait is affected by an infected devil's own tumor i or the tumor of another devil j). z_k is inherited according to the infinitesimal model of quantitative genetics while x_k evolves through mutation. We refer to z_k and x_k for a given k as a "trait pair" and the coevolution of these trait pairs serves as the focal point of our analysis. Our definitions of resistance and tolerance follow those of Råberg et al. (2009), where resistance is measured by a host's ability to limit pathogen burden (in this case by reducing within-host tumor growth or resisting infection altogether) and tolerance is measured by a host genotype's fitness as a function of pathogen burden. The full overview, design concepts, and details (ODD) protocol (Grimm et al., 2006, 2010, 2020) may be found in Supplement 1. Figure 1 provides a graphical overview of the model structure and Table 1 provides a list of variables, parameters, and notation.

Devil demographics

Devils are synchronous, annual breeders with a mating season typically lasting from late February to early April in the absence of DFTD (Hesterman, 2008; Hesterman et al., 2008; Jones et al., 2008; Pemberton, 1990). Most births occur from March to April and DFTD is not transmitted vertically (Pyecroft et al., 2007). As devils are altricial marsupials, young stay in the pouch for 4 months and the den for 6 months, usually dispersing from their natal site between December and April (Pemberton, 1990; Rose et al., 2017). Devils typically become reproductively mature at age 2, although DFTD has led to an increase in precocial female breeding at age 1 in some sites (~14 months; Jones et al., 2008; Lachish et al., 2009).

We model a simplified life history where mating occurs within a single week-long timestep, with each adult female reproducing with probability p_{mate} and multiple paternity (Russell et al., 2019). Female devils have four teats, limiting litter size to $b_{max} = 4$ offspring. Offspring survive to become independent with probability b_{prob}. Devils reproductively mature adults at age $a_{mat} = 2$ years, with no precocial breeding, last reproduce at age $a_{LR} = 5$ years, and die of old age at $a_{max} = 7$ years (Rose et al., 2017). Uninfected adults die at a rate d_A^{tot}, which is made up of a density-independent component d_{DI} and a density-dependent component $d_{DD}N$, where N is the number of devils. Subadult devils experience higher mortality rates than adults (Rose et al., 2017) such that per-capita juvenile death rate $d_{SA}^{tot} = d_{DI} + d_{SA} + d_{DD}N$ where d_{SA} is the excess subadult mortality.

Infection

DFTD is transmitted through biting during mating and competitive interactions (Hamede et al., 2008, 2013; Hamilton et al., 2019, 2020). Because the effects of DFTD on devil behavior are not this study's focus, we assume simplified interactions with no spatial or social structure and frequency-dependent contacts (as this mode of transmission is most consistent with high DFTD prevalence in spite of strong population declines; McCallum et al., 2009): A devil interacts with other devils at a constant weekly rate $r_{contact}$ and encounters infected individuals at a rate $r_{contact}\frac{N_I}{N}$.

Let $P_{ij}^{I}(t)$ be the probability of successful infection given a contact between susceptible individual i and infected individual j at time t. If infection probability, population size, and number of infected individuals are approximately constant over a week, the number of successful transmissions is Poisson distributed, and the probability that susceptible individual i remains susceptible at the start of the next week is

$$P_i^S = \exp\left[-\frac{N_I}{N} r_{contact} \bar{P}_i^I\right],$$

where $\bar{P}_i^I = \frac{1}{N_I}\Sigma_{j=1}^{N_I} P_{ij}^I$ is the average transmission probability given an infectious contact. We assume that co-infections by multiple tumors have no meaningful impact on disease progression. If multiple transmissions occur in the same week, the "first" infecting individual is randomly selected with probability $\frac{P_{ij}^I}{\Sigma_{j=1}^{N_I} P_{ij}^I}$.

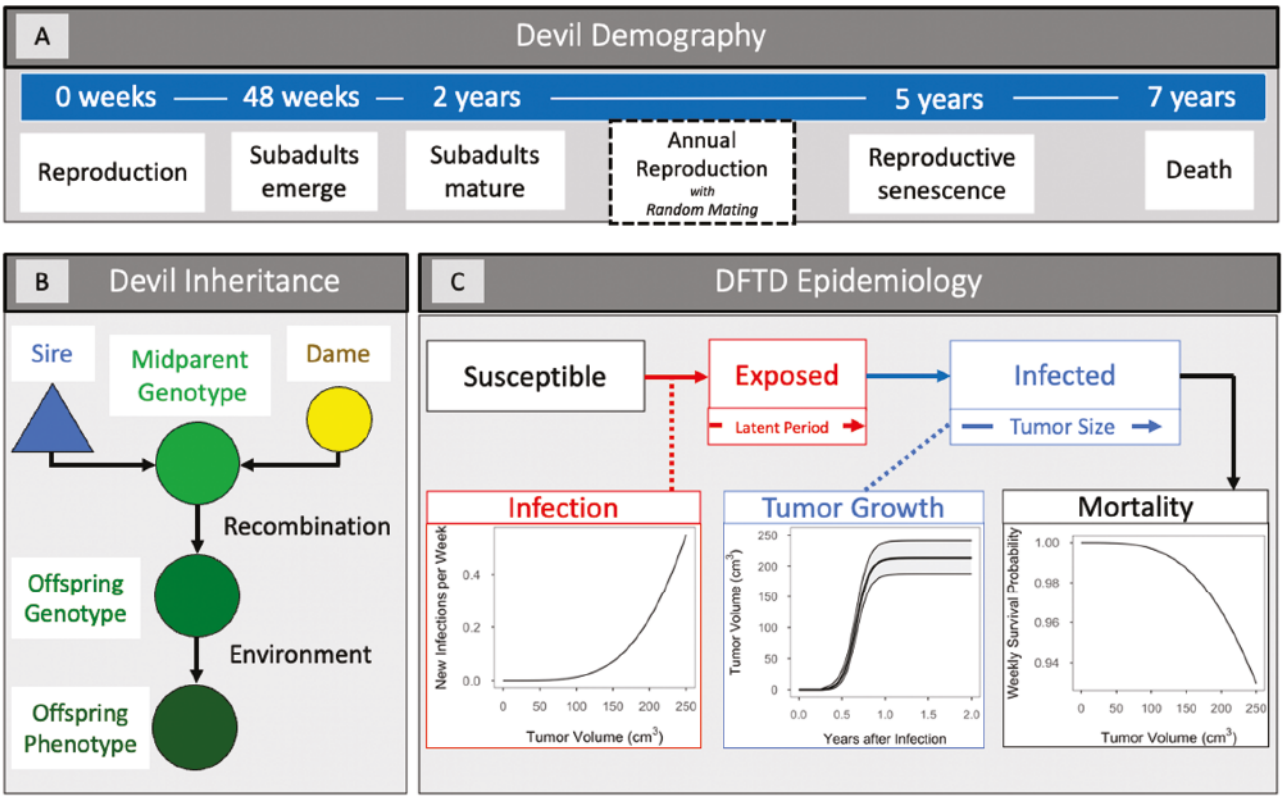

Figure 1. A visual schematic of the individual-based model. (A) The simplified Tasmanian devil life-cycle used in the model. (B) Devil inheritance, following the infinitesimal model of quantitative genetics. Colors represent the breeding values of the sire, dam, and offspring. (C) DFTD epidemiology in a susceptible-exposed-infected (SEI) framework. Transmission and mortality are both functions of tumor volume, which increases stochastically and logistically over time. Bands in the tumor growth plot represent the 95% confidence interval for tumor volume at each point in time after infection. *Note*. *DFTD* = devil facial tumor disease.

We model P^{I}_{ij} as a logistic function of the log tumor load $\ln[L_j]$ of individual j. The maximum infection probability P^{I}_{max} is modified by the resistance of individual i to infection by individual j (R_{ij}, not to be confused with the basic reproduction number R_0) which is a function of the resistance genotype $z_{1,i}$ of devil i and the transmissibility genotype $x_{1,j}$ of tumor j. We then have

$$P^{\mathrm{I}}_{ij} = P^{\mathrm{I}}_{max} R_{ij} \frac{\left(\frac{L_j}{L_l^{crit}}\right)^{\gamma}}{1 + \left(\frac{L_j}{L_l^{crit}}\right)^{\gamma}} \quad (1)$$

where L_l^{crit} is the critical tumor load at which $P^{\mathrm{I}}_{ij} = 0.5 P^{\mathrm{I}}_{max} R_{ij}$ and γ is the logistic rate parameter. Thus,

$$P^{\mathrm{S}}_i = \exp\left[-\frac{N_I}{N}\beta \hat{P}^{\mathrm{I}}_i\right], \quad (2)$$

where $\hat{P}^{\mathrm{I}}_i = \frac{\bar{P}^{\mathrm{I}}_i}{P^{\mathrm{I}}_{max}}$ and P^{I}_{max} has been combined with $r_{contact}$ to give the maximum transmission coefficient $\beta = P^{\mathrm{I}}_{max} r_{contact}$. Because observed infections are much lower for subadults (Lazenby et al., 2018) due to higher pre-puberty anti-cancer immune capacity (Cheng et al., 2017) and lack of involvement in mating interactions, we assume that the subadult infection probability is reduced, relative to the adult infection probability, by fixed subadult resistance factor R_{SA}.

Tumor growth

We model tumor growth as stochastic, following Wells et al. (2017). Tumors have a latent period (τ) between the time of infection T^I_i and the time at which they become transmissible (Espejo et al., 2022; McCallum et al., 2009). The regression of visible tumors is very rare in natural populations (Margres et al., 2020), and the expected volume $\bar{L}_i(t)$ for tumor i, measured in cm^3, increases logistically over time at genotype-dependent rate r_i^{growth} to maximum expected tumor size L_{max} (Hamede et al., 2017; Wells et al., 2017):

$$\bar{L}_i(t) = \frac{L_{max}}{1 + (L_{max} - 1)e^{-r_i^{growth}(t - T^I_i - \tau)}} - 1, \quad (3)$$

when $t \geq T^I_i + \tau$ and $L(t) = 0$ when $t < T^I_i + \tau$. We used a modified logistic growth function, with initial tumor load $L_0 = 0$, because the actual initial tumor load is small and difficult to estimate empirically. Equation 3 is approximately equal to the standard logistic curve for $L_{max} \gg 1$. We assume individual variation around $\bar{L}_i(t)$ is Gamma distributed with shape parameter $\lambda \bar{L}_i(t)$ and rate parameter λ (from Wells et al., 2017).

Mortality

Field studies demonstrate that tumor load affects body condition (Ruiz-Aravena et al., 2018) and mortality rate

Table 1. Names and mathematical notation of the model state variables and the model parameters used in parameter selection.

Variable name	Notation
Population state variables	
Time	t
Devil population size	N
Susceptible devils	N_S
Infected devils	N_I
Realized individual state variables	
Probability of devil i remaining susceptible	P_i^S
Realized resistance of devil i to infection by tumor j	R_{ij}
Tumor load on devil i	L_i
Expected tumor load	$\bar{L}_i$
Time of infection	T_i^I
Realized tumor growth rate	r_i^{growth}
Critical tumor size (mortality)	$L_{S,i}^{crit}$
Devil survival probability	P_i^{surv}
Latent individual traits	
Latent devil resistance to infection	$z_{1,i}$
Latent devil resistance to tumor growth	$z_{2,i}$
Latent devil tolerance	$z_{3,i}$
Devil phenotype vector	$\mathbf{z}$
Devil genotype vector	$\mathbf{g}$
Devil genetic covariance matrix	$\mathbf{G}(t)$
Devil segregation covariance matrix	$\mathbf{S}$
Latent tumor transmissibility	$x_{1,i}$
Latent tumor growth	$x_{2,i}$
Latent tumor virulance	$x_{3,i}$
Tumor phenotype vector	$\mathbf{x}$
Parameter name	**Notation**
Devil demographic parameters	
Probability of mating	p_{mate}
Offspring survival probability	b_{prob}
Density-dependent death rate	d_{DD}
Density-independent death rate	d_{DI}
Subadult excess death rate	d_{SA}
DFTD parameters	
Initial tumor growth rate	r_0^{growth}
Tumor growth heterogeneity	λ
Maximum tumor load	L_{max}
Tumor latent period	τ
Minimum survival probability	S_{min}
Baseline critical tumor size (mortality)	$L_{S_0}^{crit}$
Mortality shape parameter	α
Maximum Transmission	β
Critical tumor size (transmission)	L_I^{crit}
Transmission shape parameter	γ
Subadult resistance factor	R_{SA}
Covariance matrices	
Initial devil genetic covariance matrix	$\mathbf{G}(0)$
Devil environmental covariance matrix	$\mathbf{E}$
Tumor mutation covariance matrix	$\mathbf{M}$

(Wells et al., 2017). We assume for simplicity that survival probability does not differ between males and females, so that if S_∞ is the fractional reduction in survival probability caused by a very large disease load, $L_{S,i}^{crit}$ is the critical disease load at which the reduction in survival probability is halfway between 1 and S_∞, and α is the pathogenicity of the disease, we then have

$$P_i^{surv} = \left(\frac{1 + S_\infty \left(\frac{L}{L_{S,i}^{crit}} \right)^\alpha}{1 + \left(\frac{L}{L_{S,i}^{crit}} \right)^\alpha} \right) e^{-(d_{DI} + d_{DD} N)}. \quad (4)$$

Disease-related phenotypes and genetics

Genome-wide association study (GWAS) results show that a substantial proportion of variation in FOI (calculated using time from age 1 to infection as an inverse proxy; Gallinson et al., 2024) and female devil survival after infection can be explained by a small number of large-effect loci in devils (~20% and 76.5% of variation explained by an average of 2 and 4.8 single nucleotide polymorphisms, SNPs, respectively; Gallinson et al., 2024; Margres et al., 2018). However, FOI was more polygenic in tumors, and female infection status was more polygenic in devils (16% and 38.3% of variation explained by an average of ~35 and 56.1 SNPs; Gallinson et al., 2024; Margres et al., 2018). To avoid the potential complications of modeling coevolution in traits with differing genetic bases (e.g., Yamamichi & Ellner, 2016), we chose to model coevolution in a purely quantitative genetic framework.

We assume that devils and tumors exhibit genetic variation in three disease-related phenotypes: Resistance to infection R_{ij}, tumor growth r_i^{growth}, and critical disease load for survival $L_{S,i}^{crit}$. Following the phenotypic difference model of coevolution (Buckingham & Ashby, 2022; Nuismer, 2017), we model the disease-related phenotypes as functions of the difference between latent devil traits z_1, z_2, and z_3 and latent tumor traits x_1, x_2, and x_3, respectively. Resistance to infection R_{ij} is a logistic function of $z_{1,i} - x_{1,j}$,

$$R_{ij} = \frac{1}{1 + \exp\left[\omega_1 (z_{1,i} - x_{1,j})\right]}, \quad (5)$$

where ω_1 is the intensity of the coevolutionary interaction. Both the mean initial devil phenotype, $\bar{z}_1(t = 0)$, and the initial tumor phenotypes are zero so that the probability of infection for the average individual in a population first exposed to the disease is $\frac{1}{2} P_{max}^I$.

The tumor growth rate r_i^{growth} on an infected individual is

$$r_i^{growth} = \max\{r_0^{growth} - \omega_2 (z_{2,i} - x_{2,i}), 0\}, \quad (6)$$

where r_i^{growth} is the initial tumor growth rate in a naive population and ω_2 is the intensity of the coevolutionary interaction. Because tumor regression is rare (0.01% of observed infections; Margres et al., 2020), we assume that $r_i^{growth} \geq 0$.

The critical tumor size $L_{S,i}^{crit}$ of an infected devil deviates from the critical size in a DFTD-naive population $L_{S_0}^{crit}$ following the equation

$$L_{S,i}^{crit} = L_{S_0}^{crit} (1 + \omega_3 (z_{3,i} - x_{3,i})), \quad (7)$$

where ω_3 is the intensity of the coevolutionary interaction. In practice, ω_1, ω_2, and ω_3 are not unique parameters, as changing the value of ω for any trait is equivalent to rescaling

the variances of z and x for that trait (Supplement 1.7). We therefore set $\omega_1 = \omega_2 = \omega_3 = 1$.

The latent phenotype vector $\mathbf{z}_i = \{z_{1,i}, z_{2,i}, z_{3,i}\}$ for devil offspring i equals the vector of breeding values $\mathbf{g}_i$ and the environmental deviation vector $\mathbf{e}_i$:

$$\mathbf{z}_i = \mathbf{g}_i + \mathbf{e}_i. \quad (8)$$

We assume the infinitesimal model (Fisher; Barton et al., 2017; Fisher et al., 2012; Fisher, 1918) such that $\mathbf{g}_i$ is the average of the maternal ($\mathbf{g}^f$) and paternal ($\mathbf{g}^m$) breeding values plus a deviation due to recombination $\mathbf{s}_i$:

$$\mathbf{g}_i = \frac{1}{2}(\mathbf{g}_i^f + \mathbf{g}_i^m) + \mathbf{s}_i. \quad (9)$$

$\mathbf{s}_i$ and $\mathbf{e}_i$ are normally distributed with mean zero and covariance matrices S and E. In the absence of DFTD, and therefore selection, the devil genetic covariance matrix G will converge to the initial devil genetic covariance matrix G(0) = 2S (Walsh & Lynch, 2018).

If the environmental component of a tumor's phenotype is normally distributed and constant during any given infection, then it may be merged with $\mathbf{e}_i$ without loss of generality (Supplement 1.7). Tumor phenotype and genotype are therefore interchangeable. The latent genotype of a tumor on a newly infected devil is inherited asexually from the tumor on the infecting devil. Mutation and other within-tumor processes (Leathlobhair & Lenski, 2022) cause a tumor's genotype to change slightly by an amount $\mathbf{m}$ each week, such that $\mathbf{x}_i(t+1) = \mathbf{x}_i(t) + \mathbf{m}$. We assume non-directional mutation where $\mathbf{m}$ is multivariate normal with mean zero and covariance matrix M.

Parameter selection

We parameterize the model with over 20 years of published results on devil demography, density, and genetics (e.g., Cunningham et al., 2021; Lazenby et al., 2018; Margres et al., 2018) by using sampled parameter sets to calculate demographic, epidemiological, and genetic quantities for which there were empirical estimates, and retaining parameter sets that yielded values consistent with those empirical estimates. This process followed a four-step procedure described in Supplement 2. Table 1 provides a list of model parameters and their notation and Table 2 provides a list of studies upon which the parameter criteria are based. Of the 1,000,000 sampled parameter combinations, only 320 met all the criteria for inclusion in the final set, which we refer to as the "selected parameter values". Histograms of selected parameter values are given in Supplementary Figures S1–S4 and the full list of selected parameters may be found in Supplementary Data.

First, we Latin hypercube sampled 1,000,000 parameter sets from the initial range of parameters (Supplementary Tables S2 and S3; see Supplement 2 for rationale). Second, for each set of parameters, we constructed an age-structured matrix population model describing pre-disease devil demographics. We then solved for the stable age distribution of the population and retained only parameter sets in which individuals age 2+ comprised 50%–75% of the population, individuals age 3+ comprised 20%–60% of the population, and individuals age 4+ comprised 5%–20% of the population, as empirically demonstrated in 12 sampling localities with multi-year mark–recapture data (Hamede et al., 2012; Lachish et al., 2009; Lazenby et al., 2018; see Supplement 2). We then chose death rates d_{DI} and d_{DD} such that the equilibrium population size was 200 individuals, corresponding to an area of roughly 150 km^2 (Cunningham et al., 2021; Lazenby et al., 2018). Due to stochasticity, stationary population sizes ranged in the individual-based model ~170–400, consistent with empirically observed pre-DFTD densities (Cunningham et al., 2021).

Third, we calculated the survival probabilities and lifetime reproductive success (LRS) for an infected devil and the basic reproduction number (R_0) for DFTD. We retained parameter sets with R_0 between 1 and 3 (McCallum et al., 2009) and LRS below replacement (Cunningham et al., 2021). Using mortality estimates from Wells et al. (2017) (Supplementary Figure S2), we retained parameters for which 3-month survival after infection was >90%, 9-month survival was 25%–75%, and 2-year survival was <20%.

Fourth, for each remaining parameter combination, we ran 100 simulations for 20 years following the arrival of DFTD. We selected parameter combinations to ensure DFTD spread (mean DFTD prevalence in years 5–15 is >10%), devil decline (mean devil abundance in years 5–15 is <80% of initial abundance; Cunningham et al., 2021), and devil–tumor coexistence (>80% probability) within the 20-year timeframe, since the longest infected populations have survived for at least this long. We then averaged the median and quartiles of the time from age 1 to infection (the FOI proxy used by Gallinson et al., 2024), across simulations and retained only parameters in which the average first quartile was 10.8–51.9 weeks after age 1, the average median was 30.1–61.8 weeks, and the average third quartile was 37.0–94.6 weeks (Gallinson et al., 2024; see Supplement 2). For each simulation, we calculated the proportion of variance (PVE) in FOI, survival after infection, and case–control explained by the devil or tumor genotype using the R^2 values of general linear models (Supplement 2). We retained parameters for which the average PVE in FOI by devil genotype was 2.7%–20.0%, the average PVE by tumor genotype was 7.4%–10.0%, and the average PVE by their interaction was 7.5%–51.4% (Fig. 2A in Gallinson et al., 2024). We also retained parameters for which the PVE in time to death by devil genotype was <27.6% and the PVE in case–control by devil genotype was 8.8%–50.2% (Margres et al., 2018). The average PVEs in FOI by tumor genotype and average PVEs in time to death by devil genotype were far below the lower cutoffs, and we instead retained parameters above the 75th PVE percentile (across parameter combinations) for each of these quantities.

Model implementation

The individual-based simulations and parameter selection process were implemented in R version 4.3.0 (R Core Team, 2023) and C++ 20 (Stroustrup, 2013) using the Rcpp package (version 1.0.10; Eddelbuettel et al., 2023). Each post-DFTD simulation was initialized by sampling the starting devil abundance and age structure from a 1,000-year time series of a simulated DFTD-free population (with a 100-year burn-in period). Initial devil genotypes were multivariate normal with mean zero and initial devil genetic covariance matrix G(0). Ten randomly selected adults were initially infected to ensure DFTD spread. Tumor genotypes were all initialized to $\mathbf{x}_i = 0$, corresponding to "baseline" tumor transmissibility, growth rate, and virulence. Each simulation was run

Table 2. A list of studies used to derive the parameter selection criteria and a brief description of their findings.

Study	Type	Sites sampled	Sampling duration	Primary goal
Lachish et al. (2009)	Mark–recapture	Freycinet	1999–2007	Estimate changes in devil age structure, sex ratio, and breeding behavior due to DFTD.
McCallum et al. (2009)	Mark–recapture; SEI model	Fentonbury, Wisedale, Bronte, Buckland, Mt William, Freycinet	1999–2008 (varies by site)	Calculate DFTD R0; estimates DFTD prevalence and devil density; predict future DFTD prevalence and devil density.
Hamede et al. (2012)	Mark–recapture	Fentonbury, Forestier, Freycinet, West Pencil Pine	2001–2010 (varies by site)	Estimate changes in devil density, DFTD prevalence, and devil age structure due to DFTD.
Wells et al. (2017)	Bayesian hierarchical mark–recapture model	West Pencil Pine	2006–2015	Estimate tumor growth and the effect of tumor size on devil survival and fecundity.
Rose et al. (2017)	Review	NA	NA	Review devil ecology, behavior, and reproduction.
Lazenby et al. (2018)	Spotlight survey; Mark–recapture	State-wide; Bronte, Buckland, Fentonbury, Granville, Narawntapu, Kempton, Takone, Woolnorth, wukalina	1985–2016; 2004–2016 (varies by site)	Estimate changes in devil density, DFTD prevalence, and devil demography due to DFTD.
Margres et al. (2018)	Genome-wide association study (GWAS)	Fentonbury, Forestier, Freycinet, wukalina, Narawntapu, West Pencil Pine	2000–2016 (varies by site)	Estimate the contribution of devil genetic variation to variation case–control, time to infection, and survival after infection.
Cunningham et al. (2021)	Spatially explicit mark–recapture; pattern-oriented diffusion simulation; Bayesian joint-likelihood model	State-wide spotlight surveys; 15 mark–recapture sites (see Cunningham et al., 2021, Supplementary Table S2)	1999–2020 (varies by site)	Estimate and predict state-wide spread of DFTD and changes in devil density.
Gallinson et al. (2024)	Two-species genome-wide association study (Co-GWAS)	Black River, Freycinet, Takone, West Pencil Pine	2006–2020 (varies by site)	Estimate contribution of devil genetic variation, tumor variation and the interaction of the two to force of infection.

for 100 years (i.e., 50 devil generations and 5,200 weekly timesteps).

Results

The effect of genetic variation on realized trait variation

We used initial devil genetic variance and tumor mutation variance (diagonal entries of G(0) and M) as proxies for the evolvability of the latent devil and DFTD traits. Figure 2 relates devil and tumor genetic variation to variation in the realized disease-related traits. To isolate the effects of devil variation from tumor variation, and vice versa, we make the following simplifications: In the first column of Figure 2, we plot the variation in the realized traits as a function of devil genetic variation assuming that $t = 0$ (i.e., the arrival of DFTD). In the second column of Figure 2, we plot variation in the disease-related traits as a function of accumulated tumor mutation variance for long-lived (2-year-old) tumors at the arrival of DFTD ($x_i = 0$) infecting devils with phenotype $z_i = 0$. These assumptions isolate the accumulated tumor mutation variance from both devil phenotypic variance and preexisting tumor genetic variance. Analytic equations for the curves in both columns are derived in Supplement 1. The third column of Figure 2 shows variation in the disease-related traits from all sources over time. The 95% confidence bands for these panels were computed over 1,000 simulated devil–tumor pairs and included variation in devil phenotype, tumor mutation, and stochastic tumor growth (see Supplement 1). For these simulations, all parameters were set to their mean selected values.

From Figure 2, we may observe the following two patterns: First, initial devil phenotypic variation is substantial, with the mean selected parameters yielding a meaningful fraction of initial devils with low infection probability and with high survival probability (at least within a 2-year timeframe; Figure 2C, F, I). Note, however, that though Figure 2C shows cumulative infection probability flattening over time, this is most likely an artifact of discounting secondary infections. In reality, once the secondary contacts themselves become infectious, there would be a rapid increase in infection probability due to higher DFTD prevalence. Second, tumor mutation generates a meaningful amount of trait variation during a single devil generation (Figure 2B, E, H). In addition to indicating rapid accumulation of tumor genetic variance, this result also illustrates that disease-related traits may change over the course of a single infection.

Theoretical coevolutionary dynamics

We first examined the range of dynamics theoretically possible for coevolution in single devil–DFTD trait pairs. We ran 1,000 simulations for each point in a 20 × 20 grid (Figure 3) across

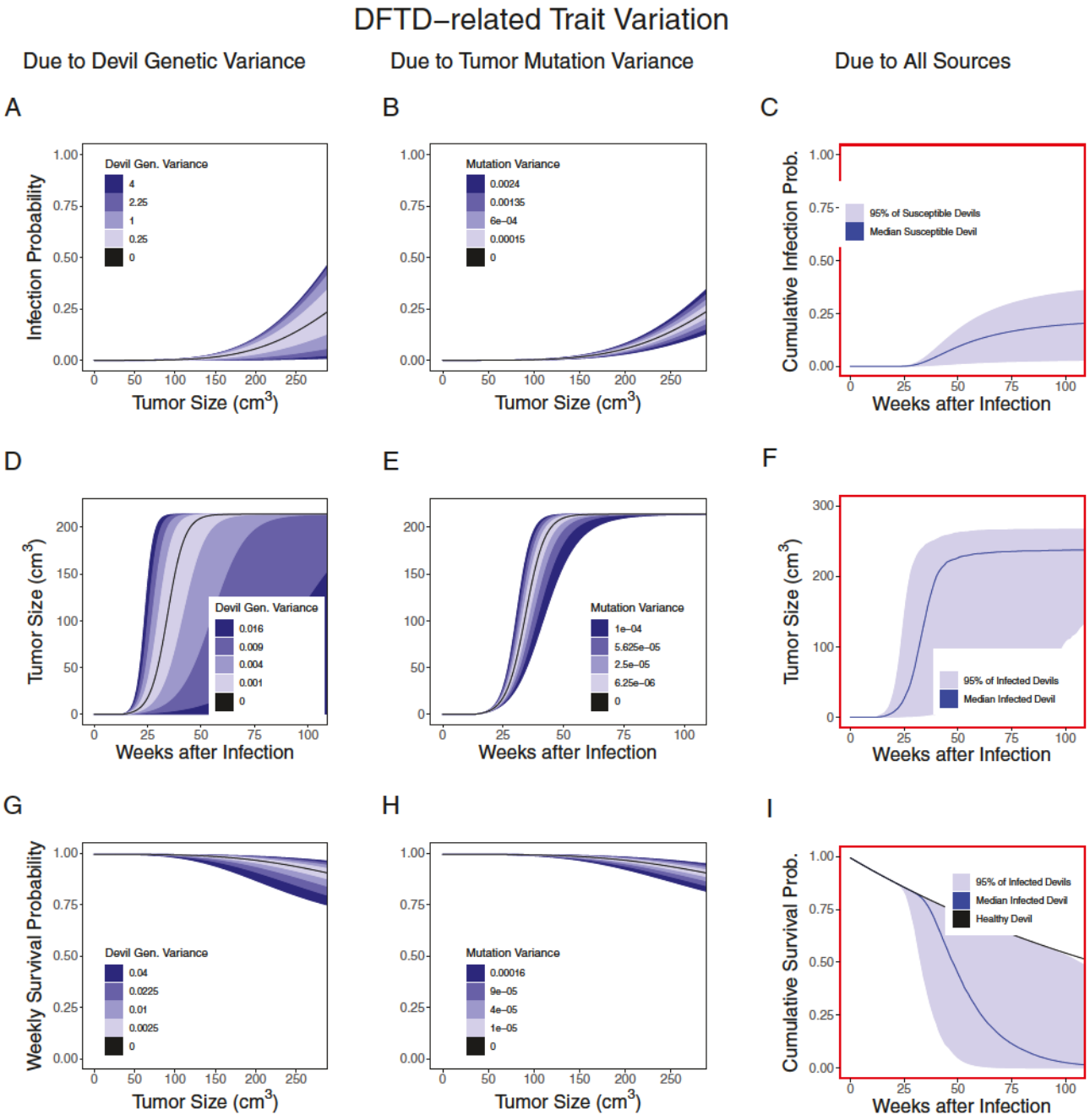

Figure 2. The relationship between initial devil genetic variance, tumor mutation variance, and variation in disease-related traits. The first column shows the variation (95% quantile bands) in disease-related traits due to devil genetic variance at the arrival of DFTD, when all tumors have the same genotype $x_{1,i} = 0$. These disease-related traits are (A) the probability of infection given contact P_{ij}^{I} as a function of tumor size, (D) tumor size (cm^3) as a function of weeks since infection, and (G) weekly survival probability as a function of tumor size. Each band represents a different value of initial devil genetic variance. The second column shows the variation (95% quantile bands) in B) the probability of infection given contact, (E) tumor size, and (H) weekly survival probability due to genetic variation among 2-year-old tumors that, after initially having the same genotype $x_{1,i} = 0$, diverged due to mutation. Each band represents a different value of DFTD mutation variance. Note that all curves in the first and second columns represent function-valued traits rather than realized values (e.g., 2-year-old tumors are unlikely to actually be less than 1 cm^3). The third column shows the variation (95% quantile bands) in disease-related traits due to all sources of variation at the arrival of DFTD. These traits are (C) the cumulative probability of infection for susceptible devils, (F) tumor growth, and (I) cumulative devil survival, all given as a function of weeks since infection. Note that panel C assumes that only the 10 initially infected devils are infectious (i.e., secondary infections are discounted) and therefore underestimates infection probability. The red boxes in column 3 indicate that the panels in this column are not directly comparable to those in columns 1 and 2. Unless otherwise specified, all parameters are set to their mean selected values. *Note. DFTD* = devil facial tumor disease.

the range of initial devil genetic variances and tumor mutation variances. For each trait pair examined, the variances of the other two trait pairs were set to zero (preventing evolution in those trait pairs) while each remaining parameter was set to the mean of its selected values (i.e., those consistent with empirical data).

When tumor transmissibility and devil resistance to infection coevolve, devil persistence depends on the relative

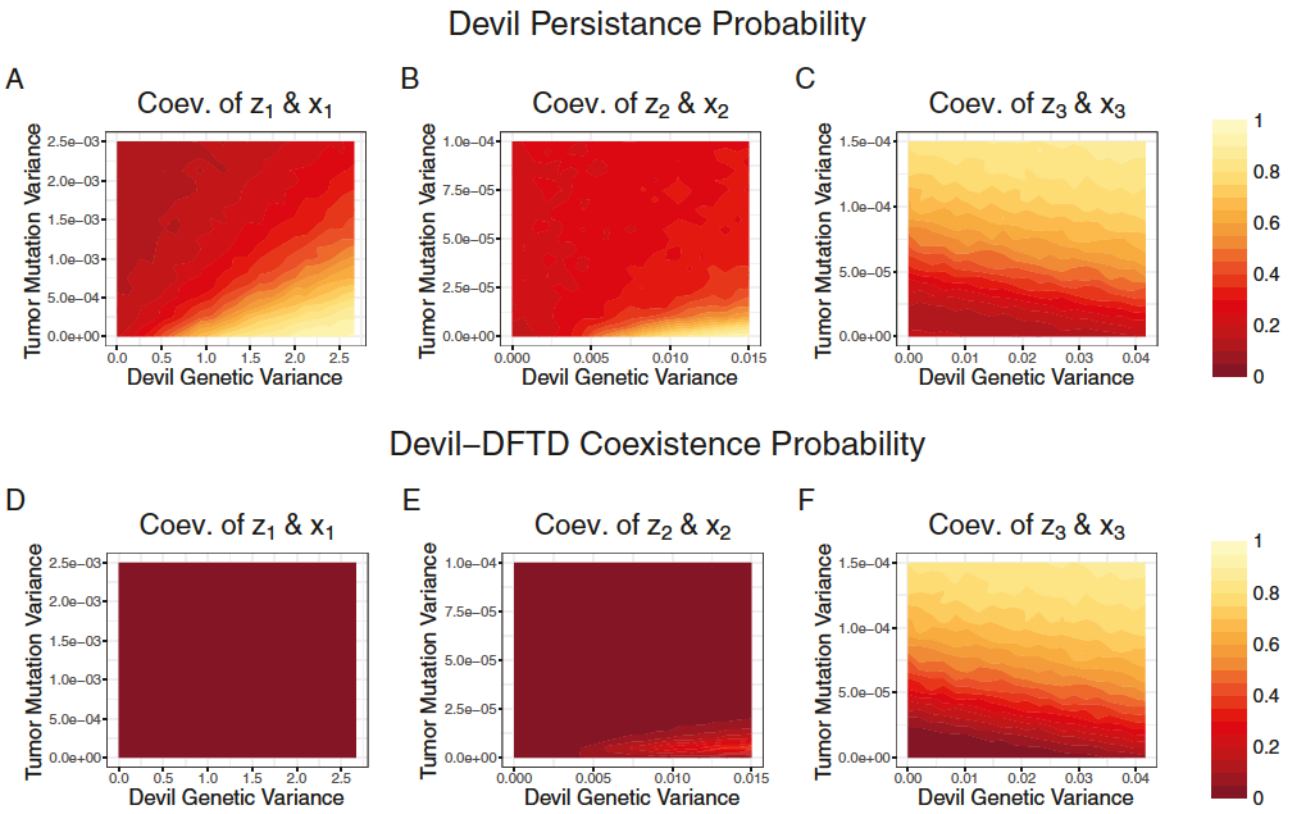

Figure 3. Devil population outcomes for coevolution in single pairs of devil–DFTD traits. Top row: the probability of devil persistence to 50 devil generations (100 years) after the introduction of the devil facial tumor disease (DFTD), for coevolution in (A) tumor transmissibility and devil resistance to infection, (B) tumor growth and devil resistance to tumor growth, and (C) tumor virulence and devil tolerance, plotted as a function of the initial genetic variation in devil resistance to infection at the arrival of DFTD (*x*-axis) and weekly tumor mutation variance in tumor transmission (*y*-axis). Bottom row: the probability of devil–DFTD coexistence to 50 devil generations for coevolution in (D) transmissibility/infection resistance, (E) tumor growth, and (F) virulence/tolerance. Probabilities are calculated over 1,000 simulated populations. Other parameters were set to their respective averages over all empirically consistent parameter values.

evolvability of devil and tumor traits (Figure 3A, D and Supplementary Figure S5A, D). Greater tumor mutation variance (faster tumor evolution) increased the likelihood of devil extirpation while greater initial devil genetic variance (faster devil evolution) increased the likelihood of tumor extirpation (Figure 3A, D). The evolutionary dynamics for fixed values of tumor mutation variance and devil genetic variance confirm simulations that ended in devil extirpation had faster DFTD evolution on average than simulations that ended in devil persistence and DFTD extirpation (Supplementary Figures S6 and S7). Greater mutation variance in tumor virulence and greater initial genetic variance in devil tolerance decreased the likelihood of devil extirpation and increased the likelihood of devil–tumor coexistence (Figure 3C, F).

Devil ecological outcomes under coevolution of tumor growth rate and devil resistance to tumor growth differ from the outcomes under coevolution of resistance to infection in several key ways (Figure 3B, E and Supplementary Figure S5B, E). First, greater tumor mutation variance had only a marginal effect on devil persistence for low values of initial devil genetic variance (<0.004). Thus, in a "tumor evolution only" scenario the relationship between tumor mutation variance and devil persistence is much flatter when tumor growth rate evolves than when tumor transmissibility evolves. Furthermore, the minimum devil persistence probability across parameters is greater under the evolution of tumor growth and devil resistance to tumor growth than under the coevolution of resistance to infection and transmissibility (16.5% compared with 9.4%). Second, the maximum probability of devil–DFTD coexistence across parameters is also far greater under coevolution of tumor growth and devil resistance to tumor growth (40.5% compared with 4.1%; Figure 3E) and the mean times to devil and DFTD extirpation are longer than under coevolution of resistance to infection and transmissibility (Supplementary Figure S5; note the different scale bars). Third, in the case of only devil evolution (Figure 3A, B near the *x*-axis), the rate of increase in devil persistence with devil genetic variance is relatively stable when resistance to infection evolves, while under the evolution of resistance to tumor growth, persistence increases relatively slowly at low variance values before sharply increasing around 0.005.

Empirically consistent coevolutionary dynamics

Second, we examined the coevolutionary dynamics of single devil–DFTD trait pairs across all selected parameter values, setting the variances of the two non-focal trait pairs zero but allowing other selected parameters to vary (i.e., each point in Figure 4 represents a different combination of all parameters). Parameter values with low devil genetic variance and high tumor mutation variance were more likely to be

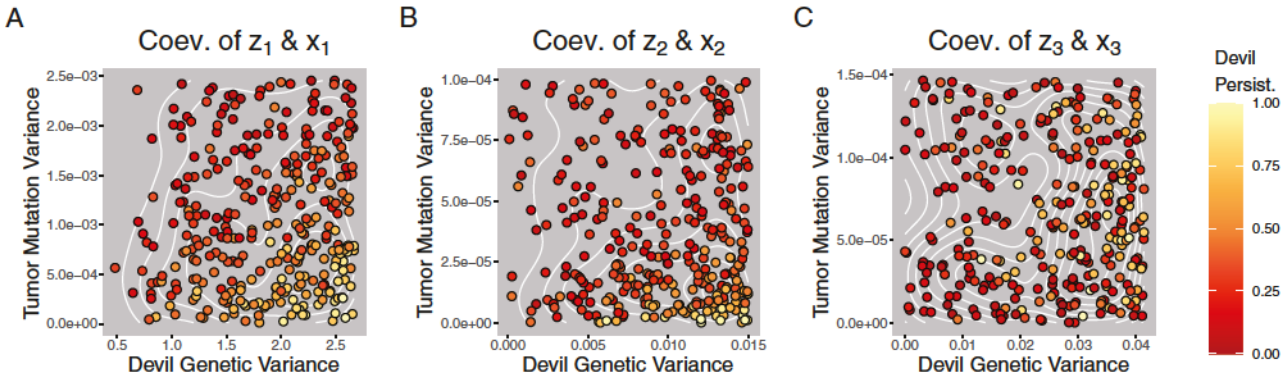

Figure 4. Empirically consistent parameter values for initial devil genetic variance and tumor mutation variance for each devil–DFTD trait pair. (A) Initial variance in devil resistance to infection at the arrival of DFTD (*x*-axis) and mutation variance in tumor transmissibility (*y*-axis). (B) Variance in devil resistance to tumor growth and in tumor growth rate. (C) Variance in devil tolerance to tumor load and in tumor virulence. Contour lines denote the density of the parameter values. Each point's color represents the probability of devil persistence, calculated over 1,000 simulated populations, for that parameter combination assuming coevolution in only the focal trait pair. *Note. DFTD* = devil facial tumor disease.

excluded during parameter selection (Figure 4A; Supplementary Figure S9). Exclusion is most pronounced for transmissibility/resistance to infection and tumor growth/resistance to tumor growth. Notably, while the selected parameter values skew heavily toward smaller values of tumor mutation variance and moderate to high values of devil genetic variance, they still encompass significant variation in devil persistence probability (Figure 4; more clearly illustrated in Supplementary Figure S9).

Devil persistence probabilities under coevolution of both transmissibility/resistance to infection and coevolution of tumor growth/resistance to tumor growth are robust to uncertainty in other model parameters (compare Figure 3A to Figure 4A and Figure 3B to Figure 4B), but are sensitive to parameter uncertainty under coevolution of virulence/tolerance. When persistence probabilities under virulence/tolerance coevolution were calculated over all selected parameter combinations rather than the mean parameter values (Supplementary Figure S9A), the average probability of devil persistence was 33.1%, and more than half (52.1%) of parameter combinations resulted in devil persistence probabilities of <25%.

Third, we examined the population and evolutionary dynamics when all three trait pairs coevolve simultaneously (Figure 5) and compared them to the dynamics when only one trait pair was allowed to coevolve (Supplementary Figures S6 and S6). To illustrate the evolutionary dynamics of each trait pair, we focus on the mean values of "net devil resistance" ($z_{1,i}-x_{1,i}$), tumor growth rate r_i^{growth} and "net devil tolerance" ($z_{3,i}-x_{3,i}$). These measures show the net effect on devil–DFTD coevolution in each trait-pair over time. In each instance, we ran 1,000 simulations with each parameter equal to its mean selected parameter value and, for the single trait-pair runs, the variances of the other two trait pairs set to zero.

When all three trait pairs coevolved simultaneously under the mean selected parameters, DFTD evolved greater transmissibility and greater tumor growth rate faster than devils evolved resistance to infection or tumor growth (Figure 5). Simultaneously, devils evolved greater tolerance and DFTD evolved reduced virulence, leading tumor prevalence to increase to an average of around 60% across simulations. There was a 74.7% probability of devil–tumor coexistence, which was strongly driven by the coevolution of reduced tumor virulence and increased devil tolerance. When only tumor transmissibility and devil resistance to infection coevolved, 78.8% of simulations resulted in devil extirpation, 21.2% showed DFTD extirpation and devil persistence, and no of simulations showed devil–DFTD coexistence (Supplementary Figure S6). Simulations in which devils persisted showed a faster evolution of devil resistance than the evolution of DFTD transmissibility, while simulations in which devils went extinct showed the opposite. When there was coevolution of tumor growth and devil resistance to tumor growth, 84.5% of simulations experienced devil extirpation (DFTD extirpation: 15.4%, devil–DFTD extirpation: 0.1%) and, for all simulations, the tumor growth rate decreased from its initial value.

Does coevolution promote devil–DFTD coexistence relative to a non-evolving population?

Finally, to quantify the global sensitivity of devil persistence, devil–DFTD coexistence, and devil recovery to coevolution in each trait pair (Figures 6 and7), we ran four sets of 1,000 simulations, for each set of selected parameters, in which either all devil and DFTD traits were allowed to coevolve or one devil–DFTD trait pair had its variances set to zero while the other two were allowed to coevolve (i.e., "leave one out"). We further ran a set of 1,000 simulations in which evolution in both devils and DFTD was entirely absent, which served as the point of comparison by which to assess the effect of coevolution. This analysis also quantified the global sensitivity of devil persistence and devil–DFTD coexistence to the total uncertainty across all model parameters (Supplementary Tables S4 and S4).

We observed a high probability of devil persistence to 50 generations (100 years) after disease introduction (median 77.0%; Figure 6A), which was was robust to parameter uncertainty (interquartile range 58.3%–91.7%); only 16.5% of parameter combinations resulted in devil persistence probabilities of <50%. We also observed a high probability of devil–DFTD coexistence. In simulations when devils persisted, DFTD had a median 74.4% chance of also persisting, corresponding to a median coexistence probability of 50.2%

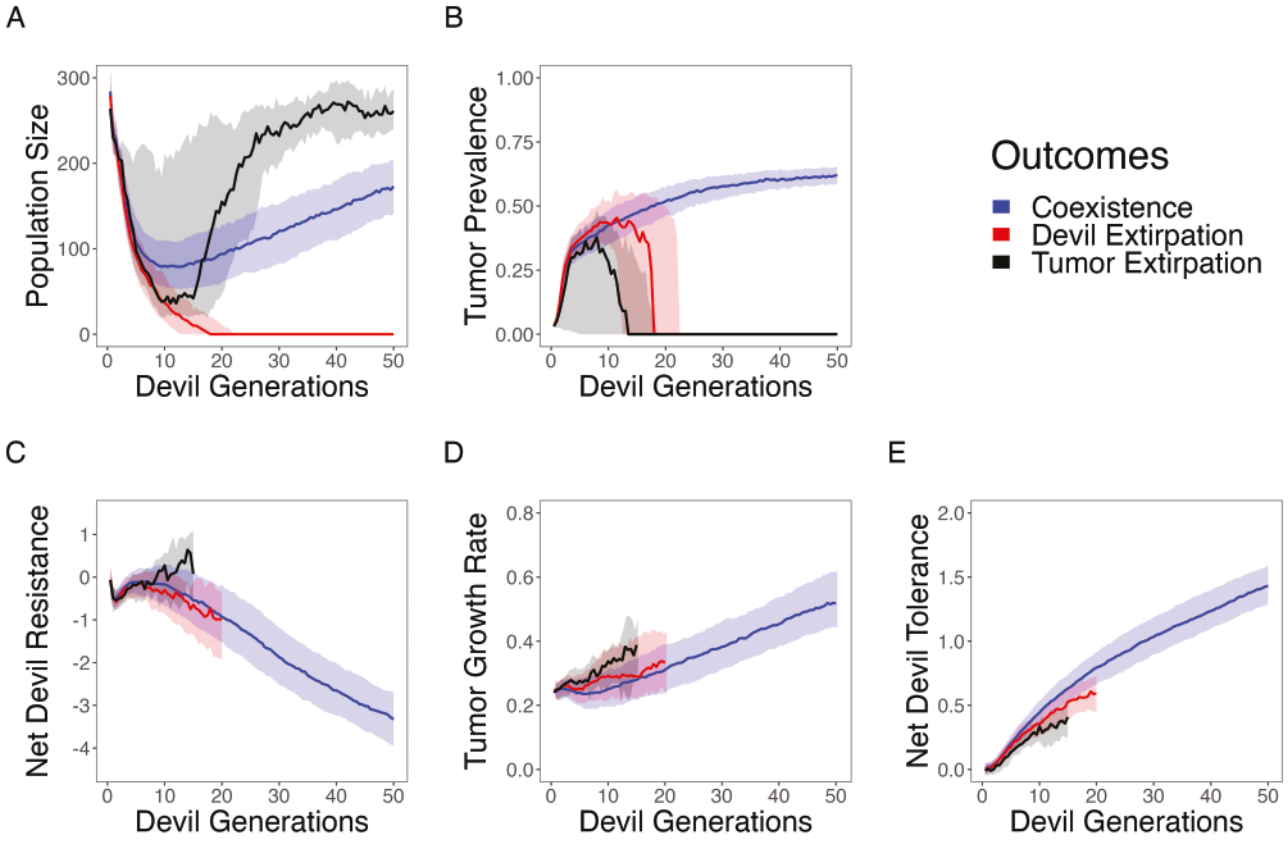

Figure 5. The dynamics of devil population size, devil facial tumor disease (DFTD) prevalence, and devil–DFTD coevolution for all three trait pairs. (A) Devil population size over 1,000 simulated populations, grouped based on population outcome. (B) DFTD prevalence. (C) Average net devil resistance, defined as the resistance phenotype of a devil minus the transmissibility phenotype of the tumor infecting it, averaged over all infected devils in the population in each year. (D) Tumor growth rate, also averaged over all infected devils in the population. (E) Average net devil tolerance, defined as the tolerance phenotype of the devil minus the virulence phenotype of the tumor infecting it. Blue denotes simulations in which both devils and DFTD persisted to 50 devil generations after the arrival of DFTD, red denotes simulations in which the devil population was extirpated, and black denotes simulations in which DFTD was extirpated. Solid lines denote the median value over time for each group of simulations and bands denote the interquartile range. Parameters were set to their respective averages over all empirically consistent parameter values.

over all simulations (Figure 6B). However, the coexistence probability was sensitive to parameter uncertainty: the probability of DFTD persistence given devil persistence had an interquartile range of 46.5%–89.8% and the overall coexistence probability had an interquartile range of 27.2%–74.4%. The median average time to devil extirpation was 36.1 years (interquartile range of 30.5–41.8 years), and the median average time to tumor extirpation was 33.8 years (interquartile range of 27.6–41.8 years). Supplementary Tables S4 and S5 give the Spearman partial correlation coefficients between each parameter, devil persistence, and devil–DFTD coexistence. For simulations in which devils and DFTD coexisted for 50 generations, devils recovered to a median, across parameters, an average of 62.0% their original population size (interquartile range: 44.7%–75.9%; Figure 7). Only 34.6% of parameter combinations had an average recovery of less than 50% for simulations with devil–DFTD coexistence (Figure 7). Parameters with the highest probability of devil–DFTD coexistence also had the highest percent recovery among simulations in which coexistence occurred (Spearman correlation = 0.588; Supplementary Figure S10). In contrast, in the absence of evolution, devil persistence was low (median 14.5%; interquartile range: 9.9%–21.5%; Supplementary Figure S9) and devil–DFTD coexistence was almost nonexistent (median: 0%; interquartile range: 0%).

Sequentially preventing the coevolution of a single trait pair while allowing the other two to coevolve (i.e., "leave one out") led to similar reductions in devil persistence probability when coevolution in transmissibility/resistance to infection and in tumor growth/resistance to tumor growth were omitted (with median persistence probabilities of 53.4% and 47.5%, respectively; Figure 6A) and a smaller reduction when coevolution of virulence/tolerance was omitted (61.6%; Figure 6A). Removing the coevolution of devil tolerance and tumor virulence dramatically decreased the probability of coexistence (median value 1.7%) while removing coevolution in tumor growth rate and transmissibility/resistance to infection led to smaller decreases (medians 30.0% and 41.75%, respectively; Figure 6B). The omission of coevolution in devil tolerance and tumor virulence also reduced the median average devil population recovery among simulations with coexistence (42.4% of initial population size; 62.8% and 61.7% with the removal of coevolution in transmissibility/resistance to infection and coevolution in tumor growth rate, respectively; Figure 7).

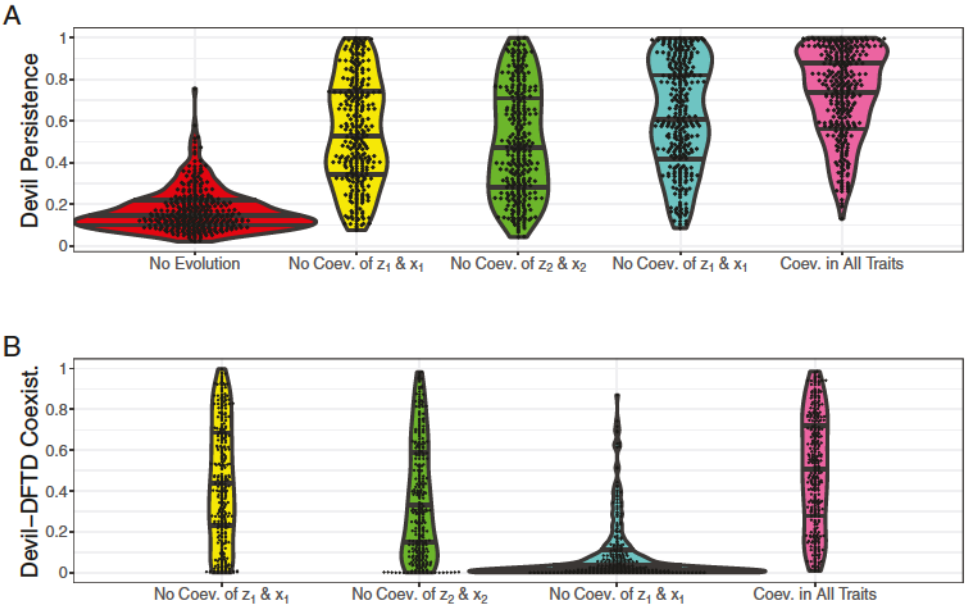

Figure 6. The distribution of probabilities of devil persistence and devil—devil facial tumor disease (DFTD) coexistence. (A) The probability of devil persistence and (B) the probability of devil–DFTD coexistence across parameter combinations when, in order from left to right, (a) There was no evolution (this plot is not included in panel B, as the probability of devil–DFTD coexistence was zero for nearly all parameter combinations), (b) Tumor transmissibility and devil resistance to infection are prevented from coevolving, but all other trait pairs are allowed to coevolve, (c) Tumor growth rate and devil resistance to tumor growth are prevented from coevolving, (d) Tumor virulence and devil tolerance are preventing from coevolving, and (e) All three trait pairs coevolve simultaneously. The lines in each violin plot represent, in ascending order, the 25th percentile, the median, and the 75th percentile of probabilities in the distribution. The probabilities of devil persistence and tumor extirpation were calculated over 1,000 simulated populations for each parameter combination and are shown within each distribution as a beeswarm plot of points.

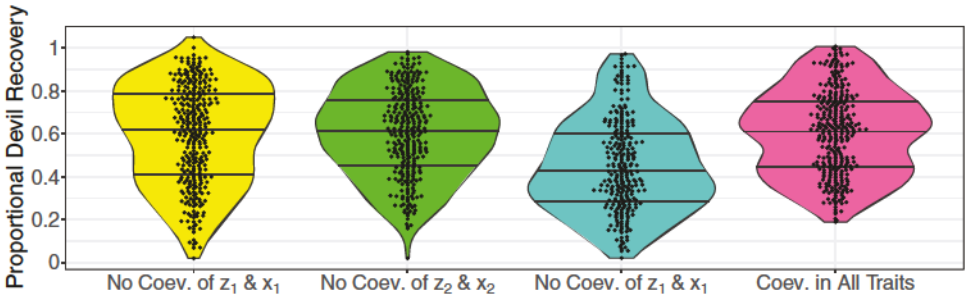

Figure 7. The average devil population recovery in the event of devil—devil facial tumor disease (DFTD) coexistence. The ratio between the final devil population size, 50 devil generations (100 years) after the arrival of DFTD, and the initial devil population size, averaged over simulations in which there was devil–DFTD coexistence. The violin plots represent, in order from left to right, scenarios where, (a) Tumor transmissibility and devil resistance to infection are prevented from coevolving, but all other trait pairs are allowed to coevolve, (b) Tumor growth rate and devil resistance to tumor growth are prevented from coevolving, (c) Tumor virulence and devil tolerance are preventing from coevolving, and (d) All three trait pairs coevolve simultaneously. The lines in each violin plot represent, in ascending order, the 25th percentile, the median, and the 75th percentile of recovery proportions across empirically consistent parameter values. Proportional devil recoveries were calculated over 1,000 simulated populations for each parameter combination and are shown within each distribution as a beeswarm plot of points. Parameter combinations in which no simulations resulted in coexistence are excluded.

Discussion

DFTD has caused declines of up to 80% in most infected Tasmanian devil populations (Cunningham et al., 2021; Lazenby et al., 2018; Storfer et al., 2018), and initial ecological models predicted devil extinction (Beeton & McCallum, 2011; McCallum et al., 2009). Nonetheless, long-diseased devil populations (>20 years) have persisted at low densities (Cunningham et al., 2021; Lazenby et al., 2018). Substantial evidence of evolution has been found in both devils and DFTD (Epstein et al., 2016; McLennan et al., 2018; Patton et al., 2020; Stahlke et al., 2021; Stammnitz et al., 2023), suggesting that coevolution may, in part, be driving continued devil persistence. To test the effect of coevolution on devil persistence, we developed one of the first models that integrates multivariate genetic coevolution with individual-based host–pathogen dynamics to predict host extinction risk. We found that empirically consistent values of genetic variance for devil traits associated with DFTD resistance and tolerance were sufficient to allow rapid devil evolution and that devil–DFTD coevolution had consistently positive effects on devil persistence relative to a non-evolving population. Multivariate coevolution led to higher probabilities, relative to previous model scenarios without evolution, of devil persistence (78.1%) and devil–DFTD coexistence (56.5%) for at least 50 devil generations (100 years), with the latter driven primarily by the evolution of greater devil tolerance and reduced

DFTD virulence. Moreover, while ecological models predict that devil–DFTD coexistence limits devil populations to, on average, 9% (Siska et al., 2018) and 48% (Wells et al., 2019) of their pre-disease abundance, we found that coevolution of devil tolerance and DFTD virulence enabled devil populations to slowly recover, despite DFTD, to an average of 60.6% of their initial abundances after 100 years, and that the degree of devil recovery was strongly correlated with the likelihood of devil–DFTD coexistence. Given that devils act ecologically as both the apex predator and scavenger in Tasmania (Cunningham et al., 2018, 2020), these differences in predicted population size could have substantial effects on the mammalian community. Taken together, these results suggest rapid devil–DFTD coevolution may have strongly contributed to continued devil persistence and will likely play an important role in shaping long-term devil–DFTD dynamics.

Coevolutionary dynamics

We modeled the coevolution of three pairs of disease-related traits: (a) tumor transmissibility and devil resistance to infection (measured by the probability of infection given contact); (b) tumor growth and devil resistance to tumor growth (measured by a tumor's logistic growth rate); (c) tumor virulence and devil tolerance (measured by the disease-related morality rate). We found very few empirical constraints on which phenotypic traits may be rapidly evolving (Figure 4), suggesting that evolution is multivariate and its effect on devil persistence is driven by the interaction between coevolving trait pairs (Figure 6; Supplementary Tables S4 and S5). Consistent with the phenotypic difference model of coevolution (Nuismer, 2017), both the coevolution of tumor transmissibility and devil resistance to infection, and the coevolution of tumor growth rate and devil resistance to tumor growth, exhibited arms race dynamics that most often led to either devil (47.8% and 33.4%) or tumor extirpation (48.8% and 37.5% of simulations, respectively, at the mean parameter values; Supplementary Figures S6 and S6). Meanwhile, the evolution of lower tumor virulence and increased devil tolerance increased both tumor prevalence and the probability of devil–DFTD coexistence (84.7%; Figure 5), consistent with theoretical predictions for the effect of virulence and tolerance evolution on disease persistence (Roy & Kirchner, 2000; reviewed in Searle & Christie, 2021).

Parameter combinations with high tumor mutation variance and low initial devil genetic variance were the most likely to generate predictions inconsistent with empirical data (Figure 4), indicating that evolutionary changes in tumor transmission and growth are unlikely to be driven by DFTD evolution alone and that devil–DFTD coevolution is likely occurring across multiple traits. Despite reduced devil genetic diversity due to historical bottlenecks (Brüniche-Olsen et al., 2014, 2016, 2018; Gooley et al. 2020; Miller et al. 2011), our results are consistent with genome-wide scans for selection and GWAS results suggesting that devils retain sufficient standing genetic variation to respond rapidly to the strong selection imposed by DFTD (Epstein et al., 2016; Fraik et al., 2020; Margres et al., 2018; Stahlke et al., 2021). Indeed, allele frequencies in SNPs associated with genes conferring antigen presentation and cell communication increase significantly in as few as four to six generations following the arrival of DFTD (Epstein et al., 2016; Fraik et al., 2020; Stahlke et al., 2021). Though variation in mutation rates between DFTD lineages (Stammnitz et al., 2023) is likely an important component of DFTD evolution, we could not use these estimates to inform our mutation variance parameters, which are expressed in phenotypic units. The empirical constraints imposed on tumor mutation variance did not constrain the range of demographic outcomes under univariate coevolution. When tumor transmissibility coevolved with devil resistance to infection, for example, the probability of devil persistence ranged from >80% to <20% (Figure 4). Thus, coevolution in any one trait pair was not sufficient to ensure devil persistence.

When either DFTD transmissibility and devil resistance to infection coevolved alone or tumor growth and devil resistance to tumor growth coevolved alone, devil traits tended to evolve faster than DFTD traits in scenarios where devils persisted, resulting in decreased probabilities of infection and slower tumor growth (Supplementary Figures S3 and S4). In contrast, when all three trait pairs coevolved, tumor growth rate and the probability of infection both increased significantly despite the evolution of increased devil resistance. It is unlikely that these increases were driven by negative correlations between devil resistance and tolerance. We did not impose any a priori assumptions on the correlation between devil traits and the only correlation with moderate support from empirical data was a positive correlation between devil resistance to tumor growth and devil tolerance (66.9% of selected parameters; Supplementary Figure S4). There was also evidence for a negative correlation between DFTD virulence and transmissibility (70.9% of selected parameters; Supplementary Figure S4), which could explain the increase in DFTD transmissibility but not the increase in growth rate (which was positively correlated with virulence for 61.7% of selected parameters). Rather, the decrease in DFTD-related devil mortality due to reduced tumor virulence and greater devil tolerance likely decreased the negative fitness consequences of DFTD for infected individuals. This result is consistent with previous models of host evolution (Restif & Koella, 2004; Singh & Best, 2021) that predict lower pathogen virulence reduces selective pressure for host resistance while increasing selective pressure for host tolerance. The evolution of reduced DFTD virulence and increased devil tolerance may therefore play a critical role in driving devil–DFTD dynamics. Indeed, female tolerance of DFTD, relative to males, has already been demonstrated, with female body condition declining by less than 5% when tumor weight reaches approximately 6% of host body mass (Ruiz-Aravena et al., 2018).

Coevolution promotes coexistence between devils and DFTD

In contrast to previous compartmental and individual-based ecological models (McCallum et al., 2009; Wells et al., 2019), we found that coevolution leads to a high probability (median: 58.9%) of devil–tumor coexistence for at least 50 generations (100 years). Devil persistence was driven by a combination of evolution in all three disease-related traits, while DFTD persistence was driven primarily by the evolution of tolerance in devils and reduced DFTD virulence (Figure 6). Though predictions of devil persistence were robust, the predicted probability of devil–DFTD coexistence was sensitive to parameter uncertainty.

Wells et al. (2019), whose model did not include evolution, reported a probability of devil extirpation similar to our

results (21% to our average 27.1% across parameters when all three trait pairs coevolve) but with higher probability of tumor extirpation (57% to our 23%) and lower probability of devil–tumor coexistence (22% to our 49.6%). This difference is likely driven by the evolution of devil tolerance and reduced DFTD virulence, as the tumor extirpation probability rises to a mean of 54.6% when the evolution of tolerance is omitted.

In contrast, the ecological model developed by Siska et al. (2018) predicted devil–DFTD coexistence at the metapopulation level for all 200 most realistic parameter combinations. They attribute this high coexistence probability to the ability of devils and DFTD to recolonize patches in the event of local extirpation, a feature not included in our model. Given typically large devil dispersal distances (i.e., genetic spatial autocorrelations suggesting 30 km on average, but up to 109 km; Lachish et al., 2011; Storfer et al., 2017) and high population connectedness (i.e., devils form only three genetic clusters across the entirety of their geographic range; Hendricks et al., 2017), possible metapopulation dynamics likely play an important role in the island-wide persistence of devils and, if included in our model, may result in a similarly high probability of devil–DFTD coexistence.

Notably, while Wells et al. (2019) and Siska et al. (2018) predict that devil–DFTD coexistence prevents devil populations from returning to their pre-disease abundance (with devils at an average of 48% and median of 9% of their pre-disease abundance, respectively) and results in population cycles (Wells et al., 2019), we find that the evolution of reduced tumor virulence and greater devil tolerance can enable devil populations to slowly recover, in spite of DFTD (we did not quantify population cycling within this broader trend). Though we found an average population recovery to 60.6% of starting abundance, recovery was strongly correlated with the probability of devil–DFTD coexistence such that selected parameters with a high probability of devil–DFTD coexistence also show a high probability of devil recovery (Spearman $\rho = 58.8$; Supplementary Figure S10).

Wells et al. (2019) also found more rapid devil and tumor extirpation, with times to devil extirpation concentrated between generations 5 and 10 (10–20 years), with a long tail, and times to tumor extirpation concentrated between generations 5 and 15 (our model predicted an interquartile range of 15–21 generations for mean time to devil extirpation and 14–21 generations for mean time to tumor extirpation). This difference likely occurred in part because we selected parameters to ensure neither devil nor DFTD extirpation occurred within the first 10 devil generations, consistent with a lack of any observed extirpation among continuously distributed wild populations (Cunningham et al., 2021).

Though we chose to model devil–DFTD coevolution in a quantitative genetic framework, selection at large-effect loci may play an important role in rapid devil–DFTD coevolution. Margres et al. (2018) found that ~7 loci explain 60.6% of genetic variation in devil tolerance. Evolution is predicted to proceed more rapidly in traits determined by a mix of large- and small-effect loci than in traits determined by small-effect loci alone, with a transient increase in genetic variance driven by the large-effect loci (Gomulkiewicz et al., 2010). It is therefore possible that parameterizing a purely quantitative genetic model with results of Margres et al. (2018) inflated our empirically plausible values of tolerance variance. However, our qualitative results are robust even if the maximum initial devil genetic variance in tolerance is halved (Supplementary Figure S11) and, while devil–DFTD coexistence correlates with devil tolerance, coexistence is more sensitive to DFTD mutation variances and correlations (Supplementary Table S5). In 2014, a second DFT strain of independent origin (DFT2) was discovered in the southeast of Tasmania. This strain originated from a male devil, as opposed to a female in the case of DFTD (James et al., 2019), has an elevated mutation rate relative to DFT1, and has already diverged into two distinct lineages (Stammnitz et al., 2023). We did not consider DFT2 in the present study, as it is believed not to have spread beyond its region of origin (James et al., 2019). However, within-host competition between disease strains can counterbalance between-host selection for reduced virulence (reviewed in Alizon et al., 2013). Therefore, if DFT2 were to spread more widely, our prediction of reduced DFTD virulence may not hold and the likelihood of devil–DFTD coexistence could be significantly affected.

Broader implications and future directions

Implications for coevolutionary theory

Our multivariate model of host-disease coevolution represents an important contribution to the theory of disease ecology and coevolution. Previous modeling studies have examined simultaneous evolution of host resistance and tolerance (Boots & Best, 2018; Boots et al., 2009; Råberg et al., 2007; Restif & Koella, 2004), evolution of pathogen virulence and transmission (Alizon et al., 2009; Cressler et al., 2016), and, separately, the coevolution of pathogen transmission and host resistance (reviewed in Buckingham & Ashby, 2022) and the coevolution of within-host pathogen growth and host immune response (Gilchrist & Sasaki, 2002). However, host-disease models that are both multivariate and coevolutionary remain rare (but see multi-step infection models such as Fenton et al., 2012; Nuismer and Dybdahl, 2016, and gene/protein network models such as Kamiya et al., 2016; Shin & MacCarthy, 2016) and, to our knowledge, our model represents one of the first to examine the effect of multivariate coevolution on host and pathogen extirpation risk. Considering coevolution in a multivariate context is important because the transmission and within-host growth of disease are multi-step processes that depend on behavioral patterns of contact, host immune responses, and the biology of the disease (reviewed in Hall et al., 2017; Handel & Rohani, 2015; McCallum et al., 2017). Selection may act on host or pathogen traits at each of these multiple steps and, as our results highlight, the traits on which selection acts may dramatically affect the host population outcome of an epizootic disease outbreak.

DFTD's slow growth and load-dependent effect on host fitness are features shared by other high-profile wildlife diseases, including chytridiomycosis in amphibians (Grogan et al., 2023; Voyles et al., 2009, 2018) and white-nose syndrome in North American bats (Blehert et al., 2009; Hoyt et al., 2021). The shape of the load-dependent infection and mortality curves has been shown to critically influence the host population persistence of both frogs and bats (Langwig et al., 2017; Wilber et al., 2017). Though there are important differences between these diseases and DFTD (such as environmental transmission and temperature-dependent growth; Hoyt et al., 2021; Wilber et al., 2017), our results

suggest that host and pathogen trait correlations are likely to play an important in these systems as well. Indeed, Wilber et al. (2024) found that evolution in each of three different host traits, analogous to the devil traits we consider, had substantially different effects on the time to host-population recovery during a chytridiomycosis outbreak.

Phenotypic tradeoffs or genetic correlations between traits are critical constraints on evolution in both hosts and pathogens (e.g., physiological or immunological costs of host resistance; Núñez-Farfán et al., 2007, resistance-tolerance tradeoffs in hosts; Boots & Best, 2018; Boots et al., 2009; Råberg et al., 2007; Restif & Koella, 2004; Singh & Best, 2021, and transmission-virulence trade-offs in pathogens, reviewed in Cressler et al., 2016) and, indeed, genetic and mutational correlations were among the parameters to which our results were most sensitive (Supplementary Table S5). In this context, it is surprising that we found evidence for a negative correlation between DFTD transmission and virulence. No study has yet examined the genetic correlation between disease-related traits in devils or DFTD and therefore the only empirical constraints on these correlation parameters in our model were likely imposed by the purely demographic selection criteria. The importance of these correlations to devil persistence emphasizes the need for continued research into the genomic basis of devil and DFTD traits and the broader need to consider rapid host-disease coevolution in a multivariate context.

Implications for devil conservation

Tasmanian devils are a charismatic species of global interest and are the focus of extensive conservation and research efforts. Early post-discovery of DFTD, a captive "insurance" population was established across zoos and wildlife parks throughout Tasmania with the aim to either reintroduce devils in cases of extirpations or supplement declining populations to enhance their genetic diversity (CBSG, 2008). Later, devils were introduced onto Maria Island, which had no prior history of Tasmanian devil presence (DPIPWE, 2010; Hogg et al., 2015, 2017). The conservation efficacy of translocating devils from this disease-free insurance population to low-density infected populations has been the subject of ongoing discussion (Hamede et al., 2021; Hohenlohe et al., 2019), with limited translocations having occurred in four natural populations (Glassock et al., 2021). Although translocation has the potential to benefit devil populations at low abundance by raising population size and potentially alleviating inbreeding depression (i.e., genetic rescue, reviewed in Grueber et al., 2019; Hedrick & Garcia-Dorado, 2016; Whiteley et al., 2015), the introduction of DFTD-naive individuals risks exacerbating the epidemic and causing outbreeding depression by disrupting the population's adaptation to DFTD (Hamede et al., 2021; Hohenlohe et al., 2019). Our predictions that coevolution promotes devil persistence and could even allow devils to regain a substantial fraction of their original abundance adds to growing evidence that translocation may not be necessary to prevent devil extinction (Cunningham et al., 2021; Wells et al., 2019). An important caveat to our result is that our model did not include inbreeding or any other Allee effect that could lead to extirpation if devil abundance drops below a minimum viable population size (Frankham et al., 2014; Luque et al., 2016). Evidence for DFTD-induced increases in devil inbreeding depression remains equivocal (Brüniche-Olsen et al., 2014; Gooley et al., 2020; Lachish et al., 2011) and the level of inbreeding depression necessary to threaten devil extinction is currently unclear. A critical next step therefore is to incorporate inbreeding into eco-evolutionary models to determine its effects on devil persistence.

Supplementary material

Supplementary material is available online at *Evolution*.

Data availability

The model scripts and output data files are available on Dryad at https://doi.org/10.5061/dryad.crjdfn3c7.

Author contributions

Conceptualization: D.T.C., A.S., R.K.H., M.E.J., M.J.M., and H.M. Data curation: D.T.C. Formal analysis: D.T.C. Methodology: all authors. Funding acquisition: A.S., R.K.H., M.E.J., M.J.M., and H.M. Resources: D.G.G., R.K.H., M.E.J., and M.J.M. Software: D.T.C. Supervision: A.S., M.E.J., H.M., M.J.M., and R.K.H. Validation: all authors. Visualization: D.T.C. Writing—original draft: D.T.C. and A.S. Writing—review and editing: all authors.

Funding

The study was funded by the National Science Foundation (https://www.nsf.gov) DEB 2027446 to M.J.M., A.S., M.E.J., and H.M. and DEB 2324456 to M.J.M., A.S., and R.K.H. R.K.H. was also supported by the Australian Research Council (https://www.arc.gov.au) ARC-DE170101116 and ADR-LP170101105, the Centre Nationale de la Recherche Scientifique (https://www.cnrs.fr/en) International Associated Laboratory Grant, the Agence National de la Recherche (https://anr.fr/en/) ANR-TRANSCAN 18-CE35-0009, and the MAVA Foundation (https://mava-foundation.org). This research used resources from the Center for Institutional Research Computing at Washington State University. The funders did not play any role in the study design, model formulation and analysis, decision to publish, or preparation of the manuscript.

Conflict of interest: The authors declare no conflict of interest.

Acknowledgments

We thank Douglas Kerlin and David Hamilton for their feedback on the formulation of the model. We also thank three anonymous reviewers for their insightful comments and suggestions.

References

Alizon, S., de Roode, J. C., & Michalakis, Y. (2013). Multiple infections and the evolution of virulence. *Ecology Letters*, *16*(4), 556–567.

Alizon, S., Hurford, A., Mideo, N., & Van Baalen, M. (2009). Virulence evolution and the trade-off hypothesis: History, current state of affairs and the future. *Journal of Evolutionary Biology*, *22*(2), 245–259.

Barton, N. H., Etheridge, A. M., & Véber, A. (2017). The infinitesimal model: Definition, derivation, and implications. *Theoretical Population Biology*, *118*, 50–73.

Beeton, N., & McCallum, H. (2011). Models predict that culling is not a feasible strategy to prevent extinction of Tasmanian devils from facial tumour disease. *Journal of Applied Ecology*, *48*(6), 1315–1323.

Berngruber, T. W., Lion, S., & Gandon, S. (2013). Evolution of suicide as a defence strategy against pathogens in a spatially structured environment. *Ecology Letters*, *16*(4), 446–453.

Blehert, D. S., Hicks, A. C., Behr, M., Meteyer, C. U., Berlowski-Zier, B. M., Buckles, E. L., Coleman, J. T., Darling, S. R., Gargas, A., Niver, R., Okoniewski, J. C., Rudd, R. J., & Stone, W. B. (2009). Bat white-nose syndrome: An emerging fungal pathogen? *Science*, *323*(5911), 227.

Bolker, B. M., Nanda, A., & Shah, D. (2010). Transient virulence of emerging pathogens. *Journal of the Royal Society Interface*, *7*(46), 811–822.

Boots, M., & Best, A. (2018). The evolution of constitutive and induced defences to infectious disease. *Proceedings of the Royal Society B: Biological Sciences*, *285*(1883), 20180658.

Boots, M., Best, A., Miller, M. R., & White, A. (2009). The role of ecological feedbacks in the evolution of host defence: What does theory tell us? *Philosophical Transactions of the Royal Society B: Biological Sciences*, *364*(1513), 27–36.

Brannelly, L. A., McCallum, H. I., Grogan, L. F., Briggs, C. J., Ribas, M. P., Hollanders, M., Sasso, T., Familiar López, M., Newell, D. A., & Kilpatrick, A. M. (2021). Mechanisms underlying host persistence following amphibian disease emergence determine appropriate management strategies. *Ecology Letters*, *24*(1), 130–148.

Brüniche-Olsen, A., Jones, M. E., Austin, J. J., Burridge, C. P., & Holland, B. R. (2014). Extensive population decline in the Tasmanian devil predates European settlement and devil facial tumour disease. *Biology Letters*, *10*(11), 20140619.

Brüniche-Olsen, A., Jones, M. E., Burridge, C. P., Murchison, E. P., Holland, B. R., & Austin, J. J. (2018). Ancient DNA tracks the mainland extinction and island survival of the Tasmanian devil. *Journal of Biogeography*, *45*(5), 963–976.

Brüniche-Olsen, A., Austin, J. J., Jones, M. E., Holland, B. R., & Burridge, C. P. (2016). Detecting selection on temporal and spatial scales: A genomic time-series assessment of selective responses to devil facial tumor disease. *PLOS ONE*, *11*(3), e0147875.

Buckingham, L. J., & Ashby, B. (2022). Coevolutionary theory of hosts and parasites. *Journal of Evolutionary Biology*, *35*(2), 205–224.

Byrne, A. Q., Vredenburg, V. T., Martel, A., Pasmans, F., Bell, R. C., Blackburn, D. C., Bletz, M. C., Bosch, J., Briggs, C. J., Brown, R. M., Catenazzi, A., Familiar López, M., Figueroa-Valenzuela, R., Ghose, S. L., Jaeger, J. R., Jani, A. J., Jirku, M., Knapp, R. A., Muñoz, A., ... Rosenblum, E. B. (2019). Cryptic diversity of a widespread global pathogen reveals expanded threats to amphibian conservation. *Proceedings of the National Academy of Sciences*, *116*(41), 20382–20387.

Carval, D., & Ferriere, R. (2010). A unified model for the coevolution of resistance, tolerance, and virulence: Resistance, tolerance, and virulence. *Evolution*, 64(10), 2988–3009.

CBSG. (2008). *Tasmanian devil PHVA final report*. Technical report, IUCN/SSC Conservation Breeding Specialist Group.

Cheng, Y., Heasman, K., Peck, S., Peel, E., Gooley, R. M., Papenfuss, A. T., Hogg, C. J., & Belov, K. (2017). Significant decline in anticancer immune capacity during puberty in the Tasmanian devil. *Scientific Reports*, *7*(1), 44716.

Cressler, C. E., McLeod, D. V., Rozins, C., Van Den Hoogen, J., & Day, T. (2016). The adaptive evolution of virulence: A review of theoretical predictions and empirical tests. *Parasitology*, *143*(7), 915–930.

Cunningham, C. X., Johnson, C. N., Hollings, T., Kreger, K., & Jones, M. E. (2019). Trophic rewilding establishes a landscape of fear: Tasmanian devil introduction increases risk-sensitive foraging in a key prey species. *Ecography, 42*(12), 2053–2059.

Cunningham, C. X., Comte, S., McCallum, H., Hamilton, D. G., Hamede, R. K., Storfer, A., Hollings, T., Ruiz-Aravena, M., Kerlin, D. H., Brook, B. W., Hocking, G., & Jones, M. E. (2021). Quantifying 25 years of disease-caused declines in Tasmanian devil populations: Host density drives spatial pathogen spread. *Ecology Letters*, *24*(5), 958–969.

De Castro, F., & Bolker, B. M. (2005a). Mechanisms of disease-induced extinction. *Ecology Letters*, *8*(1), 117–126.

De Castro, F., & Bolker, B. M. (2005b). Parasite establishment and host extinction in model communities. *Oikos*, *111*(3), 501–513.

DPIPWE. (2010). *Recovery plan for the Tasmanian devil (Sarcophilus harrisii)*. Technical report, Department of Primary Industries, Parks, Water and Environment.

Eddelbuettel, D., Francois, R., Allaire, J., Ushey, K., Kou, Q., Russell, N., Ucar, I., Bates, D., & Chambers, J. (2023). *Rcpp: Seamless R and C++ Integration. R package version 1.0.11*. Springer.

Epstein, B., Jones, M., Hamede, R. K., Hendricks, S., McCallum, H., Murchison, E. P., Schönfeld, B., Wiench, C., Hohenlohe, P., & Storfer, A. (2016). Rapid evolutionary response to a transmissible cancer in Tasmanian devils. *Nature Communications*, *7*(1), 12684.

Espejo, C., Wilson, R., Pye, R. J., Ratcliffe, J. C., Ruiz-Aravena, M., Willms, E., Wolfe, B. W., Hamede, R. K., Hill, A. F., Jones, M. E., Woods, G. M., & Lyons, A. B. (2022). Cathelicidin-3 associated with serum extracellular vesicles enables early diagnosis of a transmissible cancer. *Frontiers in Immunology*, *13*, 858423.

Fenton, A., Antonovics, J., & Brockhurst, M. A. (2012). Two-step infection processes can lead to coevolution between functionally independent infection and resistance pathways. *Evolution*, *66*(7), 2030–2041.

Fisher, M. C., Henk, D. A., Briggs, C. J., Brownstein, J. S., Madoff, L. C., McCraw, S. L., & Gurr, S. J. (2012). Emerging fungal threats to animal, plant and ecosystem health. *Nature*, *484*(7393), 186–194.

Fisher, R. A. (1918). Xv.—The correlation between relatives on the supposition of Mendelian inheritance. *Earth and Environmental Science Transactions of the Royal Society of Edinburgh*, *52*(2), 399–433.

Fraik, A. K., Margres, M. J., Epstein, B., Barbosa, S., Jones, M., Hendricks, S., Schönfeld, B., Stahlke, A. R., Veillet, A., Hamede, R. K., McCallum, H., Lopez-Contreras, E., Kallinen, S. J., Hohenlohe, P. A., Kelley, J. L., & Storfer, A. (2020). Disease swamps molecular signatures of genetic-environmental associations to abiotic factors in Tasmanian devil (*Sarcophilus harrisii*) populations. *Evolution*, *74*(7), 1392–1408.

Frankham, R., Bradshaw, C. J., & Brook, B. W. (2014). Genetics in conservation management: Revised recommendations for the 50/500 rules, red list criteria and population viability analyses. *Biological Conservation*, *170*, 56–63.

Gallinson, D. G., Kozakiewicz, C. P., Rautsaw, R. M., Beer, M. A., Ruiz-Aravena, M., Compte, S., Hamilton, D. G., Kerlin, D. H., McCallum, H., Hamede, R. K., Jones, M. E., Storfer, A., McMinds, R., & Margres, M. J. (2024). Intergenomic signatures of coevolution between Tasmanian devils and an infectious cancer. *Proceedings of the National Academy of Sciences*, *121*(12), e2307780121.

Gilchrist, M. A., & Sasaki, A. (2002). Modeling host–parasite coevolution: A nested approach based on mechanistic models. *Journal of Theoretical Biology*, *218*(3), 289–308.

Glassock, G. L., Grueber, C. E., Belov, K., & Hogg, C. J. (2021). Reducing the extinction risk of populations threatened by infectious diseases. *Diversity*, *13*(2), 63.

Gomulkiewicz, R., Holt, R. D., Barfield, M., & Nuismer, S. L. (2010). Genetics, adaptation, and invasion in harsh environments. *Evolutionary Applications*, *3*(2), 97–108.

Gooley, R. M., Hogg, C. J., Fox, S., Pemberton, D., Belov, K., & Grueber, C. E. (2020). Inbreeding depression in one of the last DFTD-free wild populations of Tasmanian devils. *PeerJ*, *8*, e9220.

Grimm, V., Berger, U., Bastiansen, F., Eliassen, S., Ginot, V., Giske, J., Goss-Custard, J., Grand, T., Heinz, S. K., Huse, G., Huth, A., Jepsen, J. U., Jørgensen C., Mooij, W. M., Müller, B., Pe'er, G., Piou, C., Railsback, S. F., Robbins, A. M., ..., & DeAngelis, D. L. (2006). A standard protocol for describing individual-based and agent-based models. *Ecological Modelling*, *198*(1–2), 115–126.

Grimm, V., Berger, U., DeAngelis, D. L., Polhill, J. G., Giske, J., & Railsback, S. F. (2010). The odd protocol: A review and first update. *Ecological Modelling*, *221*(23), 2760–2768.

Grimm, V., Railsback, S. F., Vincenot, C. E., Berger, U., Gallagher, C., DeAngelis, D. L., Edmonds, B., Ge, J., Giske, J., Groeneveld, J., Johnston, A. S. A., Milles, A., Nabe-Nielsen, J., Pohill, J. G., Radchuk, V., Rohwäder, M., Stillman, R. A., Thiele, J. C., & Ayllón, D. (2020). The odd protocol for describing agent-based and other simulation models: A second update to improve clarity, replication, and structural realism. *Journal of Artificial Societies and Social Simulation*, *23*(2), 7.

Grogan, L. F., Mangan, M. J., & McCallum, H. I. (2023). Amphibian infection tolerance to chytridiomycosis. *Philosophical Transactions of the Royal Society B: Biological Sciences*, *378*(1882), 20220133.

Grueber, C. E., Fox, S., McLennan, E. A., Gooley, R. M., Pemberton, D., Hogg, C. J., & Belov, K. (2019). Complex problems need detailed solutions: Harnessing multiple data types to inform genetic management in the wild. *Evolutionary Applications*, *12*(2), 280–291.

Hairston, N. G., Ellner, S. P., Geber, M. A., Yoshida, T., & Fox, J. A. (2005). Rapid evolution and the convergence of ecological and evolutionary time. *Ecology Letters*, *8*(10), 1114–1127.

Hall, M. D., Bento, G., & Ebert, D. (2017). The evolutionary consequences of stepwise infection processes. *Trends in Ecology & Evolution*, *32*(8), 612–623.

Hamede, R. K., Beeton, N. J., Carver, S., & Jones, M. E. (2017). Untangling the model muddle: Empirical tumour growth in Tasmanian devil facial tumour disease. *Scientific Reports*, *7*(1), 6217.

Hamede, R. K., Fountain-Jones, N. M., Arce, F., Jones, M., Storfer, A., Hohenlohe, P. A., McCallum, H., Roche, B., Ujvari, B., & Thomas, F. (2023). The tumour is in the detail: Local phylogenetic, population and epidemiological dynamics of a transmissible cancer in Tasmanian devils. *Evolutionary Applications*, *16*(7), 1316–1327.

Hamede, R. K., Lachish, S., Belov, K., Woods, G., Kreiss, A., Pearse, A., Lazenby, B., Jones, M., & McCallum, H. (2012). Reduced effect of Tasmanian devil facial tumor disease at the disease front. *Conservation Biology*, *26*(1), 124–134.

Hamede, R. K., Madsen, T., McCallum, H., Storfer, A., Hohenlohe, P. A., Siddle, H., Kaufman, J., Giraudeau, M., Jones, M., Thomas, F., & Ujvari, B. (2021). Darwin, the devil, and the management of transmissible cancers. *Conservation Biology*, *35*(2), 748–751.

Hamede, R. K., McCallum, H., & Jones, M. (2008). Seasonal, demographic and density-related patterns of contact between Tasmanian devils (*Sarcophilus harrisii*): Implications for transmission of devil facial tumour disease. *Austral Ecology*, *33*(5), 614–622.

Hamede, R. K., McCallum, H., & Jones, M. (2013). Biting injuries and transmission of Tasmanian devil facial tumour disease. *Journal of Animal Ecology*, *82*(1), 182–190.

Hamilton, D. G., Jones, M. E., Cameron, E. Z., Kerlin, D. H., McCallum, H., Storfer, A., Hohenlohe, P. A., & Hamede, R. K. (2020). Infectious disease and sickness behaviour: Tumour progression affects interaction patterns and social network structure in wild Tasmanian devils. *Proceedings of the Royal Society B: Biological Sciences*, *287*(1940), 20202454.

Hamilton, D. G., Jones, M. E., Cameron, E. Z., McCallum, H., Storfer, A., Hohenlohe, P. A., & Hamede, R. K. (2019). Rate of intersexual interactions affects injury likelihood in Tasmanian devil contact networks. *Behavioral Ecology*, *30*(4), 1087–1095.

Handel, A., & Rohani, P. (2015). Crossing the scale from within-host infection dynamics to between-host transmission fitness: A discussion of current assumptions and knowledge. *Philosophical Transactions of the Royal Society B: Biological Sciences*, *370*(1675), 20140302.

Hedrick, P. W., & Garcia-Dorado, A. (2016). Understanding inbreeding depression, purging, and genetic rescue. *Trends in Ecology & Evolution*, *31*(12), 940–952.

Hendricks, S., Epstein, B., Schönfeld, B., Wiench, C., Hamede, R. K., Jones, M., Storfer, A., & Hohenlohe, P. (2017). Conservation implications of limited genetic diversity and population structure in Tasmanian devils (Sarcophilus harrisii). *Conservation Genetics*, *18*(4), 977–982.

Hendry, A. P., & Gonzalez, A. (2008). Whither adaptation? *Biology & Philosophy*, *23*(5), 673–699.

Hendry, A. P., Schoen, D. J., Wolak, M. E., & Reid, J. M. (2018). The contemporary evolution of fitness. *Annual Review of Ecology, Evolution, and Systematics*, *49*(1), 457–476.

Hesterman, H. (2008). *Reproductive physiology of the Tasmanian devil (Sarcophilus harisii) and spotted-tailed quail (Dasyurus maculatus)* [Dissertation]. University of Tasmania.

Hesterman, H., Jones, S., & Schwarzenberger, F. (2008). Reproductive endocrinology of the largest Dasyurids: Characterization of ovarian cycles by plasma and fecal steroid monitoring. Part I. The Tasmanian devil (*Sarcophilus harrisii*). *General and Comparative Endocrinology*, *155*(1), 234–244.

Hogg, C., Lee, A., Srb, C., & Hibbard, C. (2017). Metapopulation management of an endangered species with limited genetic diversity in the presence of disease: The Tasmanian devil *Sarcophilus harrisii*. *International Zoo Yearbook*, *51*(1), 137–153.

Hogg, C. J., Ivy, J. A., Srb, C., Hockley, J., Lees, C., Hibbard, C., & Jones, M. (2015). Influence of genetic provenance and birth origin on productivity of the Tasmanian devil insurance population. *Conservation Genetics*, *16*, 1465–1473.

Hohenlohe, P. A., McCallum, H. I., Jones, M. E., Lawrance, M. F., Hamede, R. K., & Storfer, A. (2019). Conserving adaptive potential: Lessons from Tasmanian devils and their transmissible cancer. *Conservation Genetics*, *20*(1), 81–87.

Hoyt, J. R., Kilpatrick, A. M., & Langwig, K. E. (2021). Ecology and impacts of white-nose syndrome on bats. *Nature Reviews Microbiology*, *19*(3), 196–210.

Hubert, J.-N., Zerjal, T., & Hospital, F. (2018). Cancer- and behavior-related genes are targeted by selection in the Tasmanian devil (*Sarcophilus harrisii*). *PLOS ONE*, *13*(8), e0201838.

James, S., Jennings, G., Kwon, Y. M., Stammnitz, M., Fraik, A., Storfer, A., Comte, S., Pemberton, D., Fox, S., Brown, B., Pye, R., Woods, G., Lyons, B., Hohenlohe, P. A., McCallum, H., Siddle, H., Thomas, F., Ujvari, B., Murchison, E. P., ... Hamede, R. K. (2019). Tracing the rise of malignant cell lines: Distribution, epidemiology and evolutionary interactions of two transmissible cancers in Tasmanian devils. *Evolutionary Applications*, *12*(9), 1772–1780.

Jones, M. E., Cockburn, A., Hamede, R. K., Hawkins, C., Hesterman, H., Lachish, S., Mann, D., McCallum, H., & Pemberton, D. (2008). Life-history change in disease-ravaged Tasmanian devil populations. *Proceedings of the National Academy of Sciences*, *105*(29), 10023–10027.

Kamiya, T., Oña, L., Wertheim, B., & van Doorn, G. S. (2016). Coevolutionary feedback elevates constitutive immune defence: A protein network model. *BMC Evolutionary Biology*, *16*, 1–10.

Kerr, P. J. (2012). Myxomatosis in Australia and Europe: A model for emerging infectious diseases. *Antiviral Research*, *93*(3), 387–415.

Kerr, P. J., Cattadori, I. M., Liu, J., Sim, D. G., Dodds, J. W., Brooks, J. W., Kennett, M. J., Holmes, E. C., & Read, A. F. (2017). Next step in the ongoing arms race between myxoma virus and wild rabbits in Australia is a novel disease phenotype. *Proceedings of the National Academy of Sciences*, *114*(35), 9397–9402.

Kerr, P. J., Cattadori, I. M., Sim, D., Liu, J., Holmes, E. C., & Read, A. F. (2022). Divergent evolutionary pathways of myxoma virus in Australia: virulence phenotypes in susceptible and partially resistant rabbits indicate possible selection for transmissibility. *Journal of Virology*, *96*(20), e00886-22.

Kwon, Y. M., Gori, K., Park, N., Potts, N., Swift, K., Wang, J., Stammnitz, M. R., Cannell, N., Baez-Ortega, A., Comte, S., Fox, S., Harmsen, C., Huxtable, S., Jones, M., Kreiss, A., Lawrence, C., Lazenby, B., Peck, S., Pye, R., ... Murchison, E. P. (2020). Evolution and lineage dynamics of a transmissible cancer in Tasmanian devils. *PLOS Biology*, *18*(11), e3000926.

Lachish, S., McCallum, H., & Jones, M. (2009). Demography, disease and the devil: Life-history changes in a disease-affected population

of Tasmanian devils (*Sarcophilus harrisii*). *Journal of Animal Ecology*, *78*(2), 427–436.

Lachish, S., Miller, K., Storfer, A., Goldizen, A., & Jones, M. (2011). Evidence that disease-induced population decline changes genetic structure and alters dispersal patterns in the Tasmanian devil. *Heredity*, *106*(1), 172–182.

Langwig, K. E., Hoyt, J. R., Parise, K. L., Frick, W. F., Foster, J. T., & Kilpatrick, A. M. (2017). Resistance in persisting bat populations after white-nose syndrome invasion. *Philosophical Transactions of the Royal Society B: Biological Sciences*, *372*(1712), 20160044.

Lazenby, B. T., Tobler, M. W., Brown, W. E., Hawkins, C. E., Hocking, G. J., Hume, F., Huxtable, S., Iles, P., Jones, M. E., Lawrence, C., Thalmann, S., Wise, P., Williams, H., Fox, S., & Pemberton, D. (2018). Density trends and demographic signals uncover the long-term impact of transmissible cancer in Tasmanian devils. *Journal of Applied Ecology*, *55*(3), 1368–1379.

Leathlobhair, M. N., & Lenski, R. E. (2022). Population genetics of clonally transmissible cancers. *Nature Ecology & Evolution*, *6*(8), 1077–1089.

Lips, K. R., Brem, F., Brenes, R., Reeve, J. D., Alford, R. A., Voyles, J., Carey, C., Livo, L., Pessier, A. P., & Collins, J. P. (2006). Emerging infectious disease and the loss of biodiversity in a neotropical amphibian community. *Proceedings of the National Academy of Sciences*, *103*(9), 3165–3170.

Lively, C. M. (2010). An epidemiological model of host-parasite coevolution and sex: Epidemiological model of host-parasite coevolution and sex. *Journal of Evolutionary Biology*, *23*(7), 1490–1497.

Lively, C. M. (2016). Coevolutionary epidemiology: Disease spread, local adaptation, and sex. *The American Naturalist*, *187*(3), E77–E82.

Luque, G. M., Vayssade, C., Facon, B., Guillemaud, T., Courchamp, F., & Fauvergue, X. (2016). The genetic allee effect: A unified framework for the genetics and demography of small populations. *Ecosphere*, *7*(7), e01413.

Margres, M. J., Jones, M. E., Epstein, B., Kerlin, D. H., Comte, S., Fox, S., Fraik, A. K., Hendricks, S. A., Huxtable, S., Lachish, S., Lazenby, B., O'Rourke, S. M., Stahlke, A. R., Wiench, C. G., Hamede, R. K., Schönfeld, B., McCallum, H., Miller, M. R., Hohenlohe, P. A., & Storfer, A. (2018). Large-effect loci affect survival in Tasmanian devils (*Sarcophilus harrisii*) infected with a transmissible cancer. *Molecular Ecology*, *27*(21), 4189–4199.

Margres, M. J., Ruiz-Aravena, M., Hamede, R. K., Chawla, K., Patton, A. H., Lawrance, M. F., Fraik, A. K., Stahlke, A. R., Davis, B. W., Ostrander, E. A., Jones, M. E., McCallum, H., Paddison, P. J., Hohenlohe, P. A., Hockenbery, D., & Storfer, A. (2020). Spontaneous tumor regression in Tasmanian devils associated with *RASL11A* activation. *Genetics*, *215*(4), 1143–1152.

McCallum, H., Barlow, N., & Hone, J. (2001). How should pathogen transmission be modelled? *Trends in Ecology & Evolution*, *16*(6), 295–300.

McCallum, H., Fenton, A., Hudson, P. J., Lee, B., Levick, B., Norman, R., Perkins, S. E., Viney, M., Wilson, A. J., & Lello, J. (2017). Breaking beta: Deconstructing the parasite transmission function. *Philosophical Transactions of the Royal Society B: Biological Sciences*, *372*(1719), 20160084.

McCallum, H., Jones, M., Hawkins, C., Hamede, R. K., Lachish, S., Sinn, D. L., Beeton, N., & Lazenby, B. (2009). Transmission dynamics of Tasmanian devil facial tumor disease may lead to disease-induced extinction. *Ecology*, *90*(12), 3379–3392.

McKnight, D. T., Schwarzkopf, L., Alford, R. A., Bower, D. S., & Zenger, K. R. (2017). Effects of emerging infectious diseases on host population genetics: A review. *Conservation Genetics*, *18*(6), 1235–1245.

McLennan, E. A., Gooley, R. M., Wise, P., Belov, K., Hogg, C. J., & Grueber, C. E. (2018). Pedigree reconstruction using molecular data reveals an early warning sign of gene diversity loss in an island population of Tasmanian devils (Sarcophilus harrisii). *Conservation Genetics*, *19*(2), 439–450.

Miller, W., Hayes, V. M., Ratan, A., Petersen, D. C., Wittekindt, N. E., Miller, J., Walenz, B., Knight, J., Qi, J., Zhao, F., Wang, Q., Bedoya-Reina, O. C., Katiyar, N., Tomsho, L. P., Kasson, L. M., Hardie, R.-A., Woodbridge, P., Tindall, E. A., Bertelsen, M. F., ... Schuster, S. C. (2011). Genetic diversity and population structure of the endangered marsupial *Sarcophilus harrisii* (Tasmanian devil). *Proceedings of the National Academy of Sciences*, *108*(30), 12348–12353.

Nuismer, S. L. (2017). *Introduction to coevolutionary theory*. Macmillan Higher Education.

Nuismer, S. L., & Dybdahl, M. F. (2016). Quantifying the coevolutionary potential of multistep immune defenses. *Evolution*, *70*(2), 282–295.

Núñez-Farfán, J., Fornoni, J., & Valverde, P. L. (2007). The evolution of resistance and tolerance to herbivores. *Annual Review of Ecology, Evolution, and Systematics*, *38*(1), 541–566.

Patton, A. H., Lawrance, M. F., Margres, M. J., Kozakiewicz, C. P., Hamede, R. K., Ruiz-Aravena, M., Hamilton, D. G., Comte, S., Ricci, L. E., Taylor, R. L., Stadler, T., Leaché, A., McCallum, H., Jones, M. E., Hohenlohe, P. A., & Storfer, A. (2020). A transmissible cancer shifts from emergence to endemism in Tasmanian devils. *Science*, *370*(6522), eabb9772.

Pemberton, D. (1990). *Social organisation and behaviour of the Tasmanian devil, Sarcophilus harrisii* [Dissertation], University of Tasmania.

Post, D. M., & Palkovacs, E. P. (2009). Eco-evolutionary feedbacks in community and ecosystem ecology: Interactions between the ecological theatre and the evolutionary play. *Philosophical Transactions of the Royal Society B: Biological Sciences*, *364*(1523), 1629–1640.

Pyecroft, S. B., Pearse, A.-M., Loh, R., Swift, K., Belov, K., Fox, N., Noonan, E., Hayes, D., Hyatt, A., Wang, L., et al. (2007). Towards a case definition for devil facial tumour disease: What is it? *EcoHealth*, *4*, 346–351.

R Core Team. (2023). *R: A language and environment for statistical computing*. R Foundation for Statistical Computing.

Råberg, L., Graham, A. L., & Read, A. F. (2009). Decomposing health: Tolerance and resistance to parasites in animals. *Philosophical Transactions of the Royal Society B: Biological Sciences*, *364*(1513), 37–49.

Råberg, L., Sim, D., & Read, A. F. (2007). Disentangling genetic variation for resistance and tolerance to infectious diseases in animals. *Science*, *318*(5851), 812–814.

Restif, O., & Koella, J. C. (2004). Concurrent evolution of resistance and tolerance to pathogens. *The American Naturalist*, *164*(4), E90–E102.

Reznick, D. N., Losos, J., & Travis, J. (2019). From low to high gear: There has been a paradigm shift in our understanding of evolution. *Ecology Letters*, *22*(2), 233–244.

Rose, R. K., Pemberton, D. A., Mooney, N. J., & Jones, M. E. (2017). *Sarcophilus harrisii* (Dasyuromorphia: Dasyuridae). *Mammalian Species*, *49*(942), 1–17.

Roy, B. A., & Kirchner, J. W. (2000). Evolutionary dynamics of pathogen resistance and tolerance. *Evolution*, *54*(1), 51–63.

Ruiz-Aravena, M., Jones, M. E., Carver, S., Estay, S., Espejo, C., Storfer, A., & Hamede, R. K. (2018). Sex bias in ability to cope with cancer: Tasmanian devils and facial tumour disease. *Proceedings of the Royal Society B*, *285*(1891), 20182239.

Russell, T., Lane, A., Clarke, J., Hogg, C., Morris, K., Keeley, T., Madsen, T., & Ujvari, B. (2019). Multiple paternity and precocial breeding in wild Tasmanian devils, *Sarcophilus harrisii* (Marsupialia: Dasyuridae). *Biological Journal of the Linnean Society*, *128*(1), 201–210.

Saunders, G., Cooke, B., McColl, K., Shine, R., & Peacock, T. (2010). Modern approaches for the biological control of vertebrate pests: An Australian perspective. *Biological Control*, *52*(3), 288–295.

Schoener, T. W. (2011). The newest synthesis: Understanding the interplay of evolutionary and ecological dynamics. *Science*, *331*(6016), 426–429.

Searle, C. L., & Christie, M. R. (2021). Evolutionary rescue in host-pathogen systems*. *Evolution*, *75*(11), 2948–2958.

Shefferson, R. P., Mason, C. M., Kellett, K. M., Goolsby, E. W., Coughlin, E., & Flynn, R. W. (2018). The evolutionary impacts of conservation actions. *Population Ecology*, *60*(1–2), 49–59.

Shin, J., & MacCarthy, T. (2016). Potential for evolution of complex defense strategies in a multi-scale model of virus-host coevolution. *BMC Evolutionary Biology*, *16*, 1–15.

Singh, P., & Best, A. (2021). Simultaneous evolution of host resistance and tolerance to parasitism. *Journal of Evolutionary Biology*, *34*(12), 1932–1943.

Siska, V., Eriksson, A., Mehlig, B., & Manica, A. (2018). A metapopulation model of the spread of the devil facial tumour disease predicts the long term collapse of its host but not its extinction, bioRxiv, preprint: not peer reviewed. https://doi.org/10.48550/arXiv.1806.05449

Smith, T. B., Kinnison, M. T., Strauss, S. Y., Fuller, T. L., & Carroll, S. P. (2014). Prescriptive evolution to conserve and manage biodiversity. *Annual Review of Ecology, Evolution, and Systematics*, *45*(1), 1–22.

Stahlke, A. R., Epstein, B., Barbosa, S., Margres, M. J., Patton, A. H., Hendricks, S. A., Veillet, A., Fraik, A. K., Schönfeld, B., McCallum, H. I., Hamede, R. K., Jones, M. E., Storfer, A., & Hohenlohe, P. A. (2021). Contemporary and historical selection in Tasmanian devils (*Sarcophilus harrisii*) support novel, polygenic response to transmissible cancer. *Proceedings of the Royal Society B: Biological Sciences*, *288*(1951), 20210577.

Stammnitz, M. R., Gori, K., Kwon, Y. M., Harry, E., Martin, F. J., Billis, K., Cheng, Y., Baez-Ortega, A., Chow, W., Comte, S., Eggertsson, H., Fox, S., Hamede, R. K., Jones, M., Lazenby, B., Peck, S., Pye, R., Quail, M. A., Swift, K., … Murchison, E. P. (2023). The evolution of two transmissible cancers in Tasmanian devils. *Science*, *380*(6642), 283–293.

Storfer, A., Epstein, B., Jones, M., Micheletti, S., Spear, S. F., Lachish, S., & Fox, S. (2017). Landscape genetics of the Tasmanian devil: Implications for spread of an infectious cancer. *Conservation Genetics*, *18*(6), 1287–1297.

Storfer, A., Hohenlohe, P. A., Margres, M. J., Patton, A., Fraik, A. K., Lawrance, M., Ricci, L. E., Stahlke, A. R., McCallum, H. I., & Jones, M. E. (2018). The devil is in the details: Genomics of transmissible cancers in Tasmanian devils. *PLOS Pathogens*, *14*(8), e1007098.

Strickland, K., Jones, M., Storfer, A., Hamede, R., Hohenlohe, P., Margres, M., McCallum, H., Comte, S., Lachish, S., & Kruuk, L. E. (2024). Adaptive potential in the face of a transmissible cancer in Tasmanian devils, *Molecular Ecology*, e17531..

Stroustrup, B. (2013). *The C++ programming language*. Pearson Education.

Valenzuela-Sánchez, A., Schmidt, B. R., Uribe-Rivera, D. E., Costas, F., Cunningham, A. A., & Soto-Azat, C. (2017). Cryptic disease-induced mortality may cause host extinction in an apparently stable host–parasite system. *Proceedings of the Royal Society B: Biological Sciences*, *284*(1863), 20171176.

Vander Wal, E., Garant, D., Calmé, S., Chapman, C. A., Festa-Bianchet, M., Millien, V., Rioux-Paquette, S., & Pelletier, F. (2014a). Applying evolutionary concepts to wildlife disease ecology and management. *Evolutionary Applications*, *7*(7), 856–868.

Vander Wal, E., Garant, D., & Pelletier, F. (2014b). Evolutionary perspectives on wildlife disease: Concepts and applications. *Evolutionary Applications*, *7*(7), 715–722.

Voyles, J., Woodhams, D. C., Saenz, V., Byrne, A. Q., Perez, R., Rios-Sotelo, G., Ryan, M. J., Bletz, M. C., Sobell, F. A., McLetchie, S., Reinert, L., Rosenblum, E. B., Rollins-Smith, L. A., Ibáñez, R., Ray, J. M., Griffith, E. J., Ross, H., & Richards-Zawacki, C. L. (2018). Shifts in disease dynamics in a tropical amphibian assemblage are not due to pathogen attenuation. *Science*, *359*(6383), 1517–1519.

Voyles, J., Young, S., Berger, L., Campbell, C., Voyles, W. F., Dinudom, A., Cook, D., Webb, R., Alford, R. A., Skerratt, L. F., & Speare, R. (2009). Pathogenesis of chytridiomycosis, a cause of catastrophic amphibian declines. *Science*, *326*(5952), 582–585.

Vredenburg, V. T., Knapp, R. A., Tunstall, T. S., & Briggs, C. J. (2010). Dynamics of an emerging disease drive large-scale amphibian population extinctions. *Proceedings of the National Academy of Sciences*, *107*(21), 9689–9694.

Walsh, B., & and Lynch, M. (2018). *Evolution and selection of quantitative traits*. Oxford University Press.

Wells, K., Hamede, R. K., Jones, M. E., Hohenlohe, P. A., Storfer, A., & McCallum, H. I. (2019). Individual and temporal variation in pathogen load predicts long-term impacts of an emerging infectious disease. *Ecology*, *100*(3), e02613.

Wells, K., Hamede, R. K., Kerlin, D. H., Storfer, A., Hohenlohe, P. A., Jones, M. E., & McCallum, H. I. (2017). Infection of the fittest: Devil facial tumour disease has greatest effect on individuals with highest reproductive output. *Ecology Letters*, *20*(6), 770–778.

Whiteley, A. R., Fitzpatrick, S. W., Funk, W. C., & Tallmon, D. A. (2015). Genetic rescue to the rescue. *Trends in Ecology & Evolution*, *30*(1), 42–49.

Wilber, M. Q., DeMarchi, J. A., Briggs, C. J., & Streipert, S. (2024). Rapid evolution of resistance and tolerance leads to variable host recoveries following disease-induced declines. *The American Naturalist*, *203*(5), 1160–1181.

Wilber, M. Q., Knapp, R. A., Toothman, M., & Briggs, C. J. (2017). Resistance, tolerance and environmental transmission dynamics determine host extinction risk in a load-dependent amphibian disease. *Ecology Letters*, *20*(9), 1169–1181.

Yamamichi, M., & Ellner, S. P. (2016). Antagonistic coevolution between quantitative and Mendelian traits. *Proceedings of the Royal Society B: Biological Sciences*, *283*(1827), 20152926.